

Dual electroweak phase transition in the two-Higgs-doublet model with the S_3 discrete symmetry

Vo Quoc Phong^{a,b,*} and Nguyen Minh Anh^{a,b,†}

^a*Department of Theoretical Physics, University of Science, Ho Chi Minh City 70000, Vietnam*

^b*Vietnam National University, Ho Chi Minh City 70000, Vietnam*

Hoang Ngoc Long^{c,d,‡}

^c*Subatomic Physics Research Group, Science and Technology Advanced Institute,
Van Lang University, Ho Chi Minh City 70000, Vietnam*

^d*Faculty of Applied Technology, School of Technology,
Van Lang University, Ho Chi Minh City 70000, Vietnam*

In this work, dual electroweak phase transition (EWPT) consisting of two phases, is carefully studied in the two-Higgs-doublet model with the S_3 discrete symmetry. The role of S_3 here is to further separate the stages of the electroweak phase transition, compared to that of the original two-Higgs-doublet model (2HDM). The strength of the electroweak phase transition (S) in the model under consideration is large enough for the first-order EWPT, specifically $1 < S < 2.8$. The ratio between the two vacuum expectation values (VEVs), $\tan \beta = v_2/v_1$, is proven to have no effects on the strength of the phase transition. This ratio only affects the mass domain that causes the first-order phase transition. Furthermore, in this paper we will show clearly that when studying the EWPT in models of more than one scalar field that generates masses, one needs to analyze the problem of phase transition under multiple stages. In other words, the effect of the first stage of symmetry breaking to the second one, is to simplify by suggestion that vacuum expectation value of the Higgs boson responsible for the initial stage is proportional to that of the field for the next stage.

PACS numbers: 11.15.Ex, 12.60.Fr, 98.80.Cq

* vqphong@hcmus.edu.vn

† minhankhntn@gmail.com

‡ hoangngoclong@vlu.edu.vn (corresponding author)

Keywords: Spontaneous breaking of gauge symmetries, Extensions of electroweak Higgs sector, Particle-theory models (Early Universe)

CONTENTS

I. INTRODUCTION	3
II. Review on the Higgs potential and comments on EWPT in the 2HDM	5
A. The Higgs potential in the 2HDM	5
B. Higgs potential at the tree level	8
C. The masses of gauge bosons	8
D. Remarks on EWPT structure in the 2HDM	9
E. Comments on EWPT in the 2HDM	14
III. Review on the 2HDM- S_3	16
A. Particle content	16
B. Higgs potential	16
C. The soft breaking of S_3 group	17
IV. Electroweak phase transition in the 2HDM- S_3	18
A. A vital role of S_3	18
B. Structure of EWPT	19
C. The effective potential	21
D. Probing the independence of EWPT strength on $\tan \beta$	25
E. The true critical temperatures	27
F. Searching the first-order EWPT and the role of $\tan \beta$	30
V. CONCLUSION AND OUTLOOKS	35
ACKNOWLEDGMENTS	39
A. Effective action of multiscalar field models	39
References	42

I. INTRODUCTION

The *Standard Model* (SM), an outstanding achievement of physics in particular, and a memorable milestone for the scientific community in general is a systematic theory of elementary particles and their interactions. The model predicted the results of many experiments, the existence of the Higgs particle; together with the Higgs mechanism, it shows us the nature of subatomic particles. However, the model still has some shortcomings such as not being able to unify gravity, describe dark matter or small neutrino mass, etc.

One of the significant phenomena in cosmology that cannot be explained by the SM is *baryon asymmetry*, also known as matter-antimatter asymmetry. This problem explains why there is an imbalance between matter and antimatter in the universe. For a strong *first-order electroweak phase transition*, the third of Sakharov's three conditions [1], plays an important role in explaining this asymmetry. It is indeed important because this condition not only explains the thermal imbalance but also provides a link between the violation of B and CP and the other two conditions of Sakharov.

The thermal imbalance is expressed through a first-order electroweak phase transition (EWPT) which should be considered first. The SM does not have enough triggers for a first-order phase transition [2–7]. Therefore, in the beyond SM, this problem must be considered (see, for example, Refs. [8–60]). The different scenarios that can be enumerated in these references are as follows: doing high-temperature effective potential, analysis of the trigger roles of new particles, the decoupling conditions, bubble nucleations, and sphalerons.

The triggers for the EWPT can be new particles (beyond SM) or parameter corrections in SM [8–45, 47–53, 55–60]. In the SM, it is contrary to the experiment that the mass of Higgs boson must be less than 125 GeV, for a strong first-order EWPT [2–7]. In a model, if the new particles are the cause of the violent EWPT, then that model can have more than one Higgs field [8–10, 13–25, 30–39, 61–63]. Another interesting point but consistent with the physical nature, the strength of EWPT is gauge-independent [40–42, 63, 64]. The self-energy term or daisy loops cause a problem for effective potentials at high temperatures. However, it is not the main trigger for EWPT and it reduces the strength of EWPT [65].

By making sure that the C and CP violations exist, the third condition of baryogenesis is given as $\Gamma_{sph} \sim \mathcal{A}(T)\exp\left(\frac{-E_{sph}}{T}\right) \ll H_{rad}$ [66–69] in the context of topological transitions, where Γ_{sph} and E_{sph} are the sphaleron rate and energy, respectively, H_{rad} is the Hubble

expansion rate in the radiation-dominated period, and $\mathcal{A}(T) \approx T^4$. This is referred to as the sphaleron decoupling situation. This condition is frequently written as $S = v_c/T_c > 1$ in the SM using the approximation $E_{sph}(T) \approx [v(T)/v]E_{sph}(T=0)$ [46–48, 70]. However, this approximation should be used with caution in models that go beyond the SM.

Through the above brief summaries, one has another aspect of EWPT survey. Currently, there are two scenarios as follows: the first one is that the EWPT process has only one stage; the second is that this process has two or three stages. Some of the theoretical models that study one stage of EWPT are the SM, Zee-Babu [63], SMEFT [71], SM with corrections to the Yukawa interaction for quarks [72, 73]. Models that study more than one stage of EWPT are the ones that consist of more than one Higgs field. Some of them are as follows: 3-3-1 models [8, 25, 74], 2-2-1 model [75].

However, there is one quite special model, the 2HDM has two vacuum expectation values (VEVs) having values/ranges in the electroweak scale. In this paper, the ways of studying the EWPT with only one stage of this model will be reconsidered. Then the strengths and weaknesses of it will be analyzed. At the same time, there are many interesting versions of the model that go beyond itself, in which there is a model of two Higgs doublets with symmetry of S_3 . This symmetry can account for quark mixing [76–78]. The S_3 symmetry has been proposed as the basic flavor symmetry in various frameworks. This discrete symmetry in the lepton sector is to produce a $\mu-\tau$ symmetry [79–82] or a tribimaximal neutrino mixing matrix [83, 84]. In the quark sector, this symmetry can produce Fritzsch and Fritzsch mass textures [85]. In addition, the nearest neighbor interactions (NNI) mass texture is hidden in a S_3 flavor symmetry [86]. Therefore, the model with S_3 is interesting, since S_3 would simplify the Higgs sector, which is very important in studying EWPT. Furthermore, since there are only two VEVs, our work of studying the multi-stages of the 2HDM- S_3 would be relatively easier compared to that of the SM.

The two-Higgs-doublet model with S_3 symmetry (2HDM- S_3) [87], one of the extended versions of the 2HDM, that has the potential to "possess" a strongly first-order electroweak phase transition, because of the following factors: the model has the heavy Higgs boson, as well as the charged Higgs boson; at the same time, it obeys the smallest non-Abelian discrete symmetry group.

More specifically, we will consider whether the first-order phase transition in the 2HDM- S_3 is strong or not. And when it is strong, the range of values of the phase transition

strength and the mass of the new particles and related parameters will be investigated.

The paper has the following structure. Except for the Introduction (Sec. I) and the Conclusion and Outlooks (Sec. V), Appendix A and Sec. II give a quick review of the effective potentials, as well as some comments and remarks on the electroweak phase transition in the 2HDM. In Sec. III and Sec. IV, the electroweak phase transition in the 2HDM- S_3 is studied. More specifically, the effective potential of the dual electroweak phase transition will be studied, the strength of first-order phase transition, the mass domain for the first-order phase transition, all of which will be given with a parameter a that will be introduced to replace the popular parameter $\tan\beta = v_2/v_1$.

II. REVIEW ON THE HIGGS POTENTIAL AND COMMENTS ON EWPT IN THE 2HDM

A. The Higgs potential in the 2HDM

The fermion and scalar spectrum with their assignments under the $SU(2)_L \times U(1)_Y$ gauge group are given by [88, 89]:

$$\begin{aligned} L_a &= \begin{pmatrix} \nu_{aL} \\ e_{aL} \end{pmatrix} \sim (2, -1), \quad Q_{aL} = \begin{pmatrix} u_{aL} \\ d_{aL} \end{pmatrix} \sim \left(2, \frac{1}{3}\right), \\ e_{aR} &\sim (1, -2), \quad u_{aR} \sim \left(1, \frac{4}{3}\right), \quad d_{aR} \sim \left(1, -\frac{2}{3}\right), \quad a = 1, 2, 3, \\ \Phi_i &= \begin{pmatrix} \phi_i^+ \\ \phi_i^0 \end{pmatrix} \sim (2, 1), \quad \langle \Phi_i \rangle = \frac{1}{\sqrt{2}} \begin{pmatrix} 0 \\ v_i \end{pmatrix} \sim (2, 1), \quad i = 1, 2. \end{aligned} \quad (1)$$

For details of the quark sector of different types of the 2HDM, the reader is referred to Refs. [88, 89]. In the 2HDM, the charge operator is defined as

$$Q = T_3 + \frac{Y}{2}. \quad (2)$$

The most general form of the effective potential in the 2HDM contains 14 parameters, and there may exist the CP conservation (charge and mirror symmetry), CP violation, and charge violation. When expressing the form of the potential, we must be careful in defining the quantities and distinguishing the parameters, since when applying the group rotations, the physics can be changed. However, in the studies of the phenomenology of the

2HDM, assumptions are often made to simplify the calculations. For example, CP is often assumed to be conserved in the Higgs fields (only then can we distinguish the scalar field from the scalar pseudo-field). Now, the CP discrete symmetry will eliminate all the fourth power terms that contain the odd number of one of two Higgs fields from the potential (for instance, $\Phi_1^\dagger \Phi_1 \Phi_1^\dagger \Phi_2$). We can also assume that all of the parameters corresponding to the fourth power terms are of real number, including the term added to break the symmetries.

With the above assumptions, putting in the symmetry Z_2 ($\Phi_1 \rightarrow \Phi_1, \Phi_2 \rightarrow -\Phi_2$) in order not to have FCNC at the tree level. After this, the most general form for the scalar potential for the two doublets Φ_1 and Φ_2 with supercharge +1 would have the following form [90]:

$$V = \mu_{11}^2 \Phi_1^2 + \mu_{22}^2 \Phi_2^2 - \mu_{12}^2 (\Phi_1 \cdot \Phi_2 + \Phi_2 \cdot \Phi_1) + \frac{\lambda_1}{2} \Phi_1^4 + \frac{\lambda_2}{2} \Phi_2^4 + \lambda_3 \Phi_1^2 \Phi_2^2 + \lambda_4 (\Phi_1 \cdot \Phi_2) (\Phi_2 \cdot \Phi_1) + \frac{\lambda_5}{2} (\Phi_1^4 + \Phi_2^4), \quad (3)$$

where we have denoted $\Phi_i^2 = \Phi_i^\dagger \Phi_i, i = 1, 2$ and $\Phi_i \cdot \Phi_j = \Phi_i^\dagger \Phi_j, i \neq j$. All the parameters $\mu_{11}, \mu_{22}, \lambda_i$ ($i = 1, \dots, 5$) are all real and the term containing μ_{12} “softly” breaks the symmetry Z_2 . Following this, there are two complex scalar doublets $SU(2)$ containing eight fields,

$$\Phi_a = \begin{pmatrix} \Delta_a^+ \\ \frac{1}{\sqrt{2}}(v_a + \rho_a + i\eta_a) \end{pmatrix}, \quad a = 1, 2. \quad (4)$$

Three of them are Goldstone bosons eaten by the massive gauge bosons W^\pm and Z^0 to generate their masses. The other five are physical scalar Higgs fields, including one scalar carrying charge, two neutral scalars, and one pseudo scalar.

Averaging over the whole space, VEVs read

$$\langle \Phi_1 \rangle_0 = \frac{1}{\sqrt{2}} \begin{pmatrix} 0 \\ v_1 \end{pmatrix}, \langle \Phi_2 \rangle_0 = \frac{1}{\sqrt{2}} \begin{pmatrix} 0 \\ v_2 \end{pmatrix}, \quad (5)$$

One of the most important parameters of the model is as follows:

$$\tan \beta = \frac{s_\beta}{c_\beta} = \frac{v_2}{v_1}, \quad (6)$$

where we have used the notations $s_\beta \equiv \sin \beta, c_\beta \equiv \cos \beta$. Here β is the rotational angle when normalizing the squared mass matrix of the charged and pseudoscalars.

Two general neutral even CP states ρ_1 and ρ_2 are not physical mass states. The mass matrix corresponding to them can be diagonalized by a rotation of a mixed angle of ρ_1 and ρ_2 .

Having two minima as above inserted into the Lagrangian which contains the mass terms corresponding to the scalar fields. First, the term that corresponds to the charged scalar field is

$$\mathcal{L}_{\phi^\pm, mass} = [\mu_{12}^2 - (\lambda_4 + \lambda_5)v_1v_2] \begin{pmatrix} \Delta_1^- & \Delta_2^- \end{pmatrix} \begin{pmatrix} \tan \beta & -1 \\ -1 & \coth \beta \end{pmatrix} \begin{pmatrix} \Delta_1^+ \\ \Delta_2^+ \end{pmatrix}. \quad (7)$$

After diagonalizing the above mass matrix, the squared mass of the charged Higgs particle,

$$m_{H^\pm}^2 = \left(\frac{\mu_{12}^2}{v_1v_2} - \lambda_4 - \lambda_5 \right) (v_1^2 + v_2^2) = \left(\frac{\mu_{12}^2}{v_1v_2} - \lambda_4 - \lambda_5 \right) v^2. \quad (8)$$

Next, the mass term that corresponds to the pseudoscalar field,

$$\mathcal{L}_{\eta, mass} = \left(\frac{\mu_{12}^2}{v_1v_2} - \lambda_5 \right) \begin{pmatrix} \eta_1 & \eta_2 \end{pmatrix} \begin{pmatrix} v_2^2 & -v_1v_2 \\ -v_1v_2 & v_1^2 \end{pmatrix} \begin{pmatrix} \eta_1 \\ \eta_2 \end{pmatrix}. \quad (9)$$

The physical squared mass of the pseudoscalar after normalization,

$$m_A^2 = \left(\frac{\mu_{12}^2}{v_1v_2} - 2\lambda_5 \right) (v_1^2 + v_2^2). \quad (10)$$

Finally, the mass term that corresponds to the remaining two scalar fields is

$$\mathcal{L}_{\rho, mass} = - \begin{pmatrix} \rho_1 & \rho_2 \end{pmatrix} \begin{pmatrix} \mu_{12}^2 \frac{v_2}{v_1} + \lambda_1 v_1^2 & -\mu_{12}^2 + \lambda_{345} v_1 v_2 \\ -\mu_{12}^2 + \lambda_{345} v_1 v_2 & \mu_{12}^2 \frac{v_1}{v_2} + \lambda_2 v_2^2 \end{pmatrix} \begin{pmatrix} \rho_1 \\ \rho_2 \end{pmatrix}. \quad (11)$$

With $\lambda_{345} = \lambda_3 + \lambda_4 + \lambda_5$, after normalizing the matrix in Eq.(11), the squared masses of the light (h) and the heavy (H) Higgs particles are, respectively:

$$\begin{aligned} m_h^2 &= \frac{1}{2} \left[(\lambda_1 v_1^2 + \lambda_2 v_2^2) + \mu_{12}^2 \frac{v^2}{v_1 v_2} \right] \\ &\quad - \sqrt{\left[\frac{\lambda_1 v_1^2 - \lambda_2 v_2^2}{2} - \frac{\mu_{12}^2}{2v_1 v_2} (v_1^2 - v_2^2) \right]^2 + (\lambda_{345} v_1 v_2 - \mu_{12}^2)^2}, \\ m_H^2 &= \frac{1}{2} \left[(\lambda_1 v_1^2 + \lambda_2 v_2^2) + \mu_{12}^2 \frac{v^2}{v_1 v_2} \right] \\ &\quad + \sqrt{\left[\frac{\lambda_1 v_1^2 - \lambda_2 v_2^2}{2} - \frac{\mu_{12}^2}{2v_1 v_2} (v_1^2 - v_2^2) \right]^2 + (\lambda_{345} v_1 v_2 - \mu_{12}^2)^2}, \end{aligned} \quad (12)$$

From the Eqs. (8), (10), (12), the squared masses of the Higgs particles always contain in them troublesome mixing terms of VEVs. A quantity is introduced as follows:

$$M_{Higgs}^2(v_1, v_2) = m_H^2 H^2 + m_h^2 h^2 + m_A^2 A^2 + m_{H^\pm}^2 (H^\pm)^\dagger H^\pm. \quad (13)$$

B. Higgs potential at the tree level

From the Higgs potential given in Eq. (3), V_0 in a form that is dependent on the VEVs as follows:

$$V_0(v_1, v_2) = \frac{\mu_{11}^2}{2}v_1^2 + \frac{\mu_{22}^2}{2}v_2^2 - \frac{\mu_{12}^2}{2}v_1v_2 + \left(\frac{\lambda_1}{8} + \frac{\lambda_5}{8}\right)v_1^4 + \left(\frac{\lambda_2}{8} + \frac{\lambda_5}{8}\right)v_2^4 + \left(\frac{\lambda_3}{4} + \frac{\lambda_4}{4}\right)v_2^2v_1^2. \quad (14)$$

$V_0(v_1, v_2)$ has a quartic form like in the SM. On the other hand, by developing the Higgs potential Eq. (3), two minimum equations which permit us to transform the mixing between v_1 and v_2 ,

$$\begin{aligned} \frac{\partial V}{\partial v_1} &= 0, \mu_{11}^2v_1 - \mu_{12}^2v_2 + (\lambda_1 + \lambda_5)\frac{v_1^3}{2} + (\lambda_3 + \lambda_4)\frac{v_2^2v_1}{2} = 0. \\ \frac{\partial V}{\partial v_2} &= 0, \mu_{22}^2v_2 - \mu_{12}^2v_1 + (\lambda_2 + \lambda_5)\frac{v_2^3}{2} + (\lambda_3 + \lambda_4)\frac{v_2v_1^2}{2} = 0. \end{aligned} \quad (15)$$

From Eq. (15), a relationship between VEVs, such as

$$\mu_{22}^2v_2^2 + (\lambda_2 + \lambda_5)\frac{v_2^4}{2} = \mu_{12}^2v_1v_2 - (\lambda_3 + \lambda_4)\frac{v_2^2v_1^2}{2}. \quad (16)$$

Substituting Eqs. (16) into Eq. (14) yields

$$V_0(v_1, v_2) = \frac{\mu_{11}^2}{2}v_1^2 + \left(\frac{\lambda_1}{8} + \frac{\lambda_5}{8}\right)v_1^4 - \left(\frac{\lambda_2}{8} + \frac{\lambda_5}{8}\right)v_2^4 = V_0(v_1) + V_0(v_2), \quad (17)$$

where $V_0(v_1) = \frac{\mu_{11}^2}{2}v_1^2 + \left(\frac{\lambda_1}{8} + \frac{\lambda_5}{8}\right)v_1^4$ and $V_0(v_2) = \left(-\frac{\lambda_2}{8} - \frac{\lambda_5}{8}\right)v_2^4$ are in the quartic form. In addition, there are alternative ways to arrive Eq. (17) which has other forms but $V_0(v_1)$ and $V_0(v_2)$ are still in the quartic form.

If the potential at the tree level had the quartic form of each vacuum expectation value, that is there are no mixing terms in it, the job of calculating the effective potential for each VEV would be much easier. This will be made clear in the following sections.

C. The masses of gauge bosons

In order to find the gauge boson masses, we starting from the kinetic term of the Higgs fields. In the 2HDM- S_3 , there are two components in the kinetic term for the two Higgs doublets,

$$\mathcal{L}_{mass}^{GB} = (\mathcal{D}_\mu \langle \Phi_1 \rangle)^\dagger (\mathcal{D}^\mu \langle \Phi_1 \rangle) + (\mathcal{D}_\mu \langle \Phi_2 \rangle)^\dagger (\mathcal{D}^\mu \langle \Phi_2 \rangle) \equiv A + B, \quad (18)$$

in which, the covariant derivatives act on Φ_1 and Φ_2 . as follows

$$\mathcal{D}^\mu = \partial^\mu - igW_i^\mu T_i - \frac{i}{2}g'B^\mu Y. \quad (19)$$

Note that the gauge fields (W_i^μ, B^μ) inside the covariant derivatives of A and B are the same. So after diagonalizing, the gauge fields in A and B are the same, and gauge bosons γ, Z, W^\pm are inferred.

From the term A , one obtains the mass components of the physical gauge bosons only depends on v_1 ,

$$M_{bosons}^A = m_{W^\pm}^2(v_1)W_\mu^+W^{-\mu} + m_Z^2(v_1)Z_\mu Z^\mu. \quad (20)$$

From the term B , one obtains the mass components of the physical gauge bosons that only depend on v_2 ,

$$M_{bosons}^B = m_{W^\pm}^2(v_2)W_\mu^+W^{-\mu} + m_Z^2(v_2)Z_\mu Z^\mu. \quad (21)$$

Therefore the bosons masses can be split into two parts,

$$m_{gauge-boson}^2(v_1, v_2) = m_{boson}^2(v_1) + m_{boson}^2(v_2). \quad (22)$$

Similar arguments for the problem can be found in Ref. [25].

D. Remarks on EWPT structure in the 2HDM

The Higgs and gauge boson sectors from the full Higgs Lagrangian,

$$\mathcal{L} = \mathcal{L}_{mass}^{GB} - V(\Phi_1, \Phi_2), \quad (23)$$

where $V(\Phi_1, \Phi_2)$ is given by Eq. (3).

Expanding the Higgs fields Φ_1 and Φ_2 around their VEVs which are v_1, v_2 , yields

$$\begin{aligned} \mathcal{L} = & \frac{1}{2}\partial^\mu v_1 \partial_\mu v_1 + \frac{1}{2}\partial^\mu v_2 \partial_\mu v_2 - V_0(v_1, v_2) + M_{gauge-bosons}^A + M_{gauge-bosons}^B \\ & + M_{Higgs}^2(v_1, v_2) + [m_{top-quark}(v_1) + m_{top-quark}(v_2)]t\bar{t}. \end{aligned} \quad (24)$$

Therefore, from the Lagrangian in Eq. (24), two motion equations according to v_1 and v_2 are calculated,

$$\partial^\mu v_1 \partial_\mu v_1 - \frac{\partial V_0(v_1)}{\partial v_1} + \sum \frac{\partial m_{bosons}^2(v_1)}{\partial v_1} W^\mu W_\mu + \frac{\partial m_{top}(v_1)}{\partial v_1} t\bar{t} + \frac{\partial M_{Higgs}^2(v_1, v_2)}{\partial v_1} = 0, \quad (25)$$

$$\partial^\mu v_2 \partial_\mu v_2 - \frac{\partial V_0(v_2)}{\partial v_2} + \sum \frac{\partial m_{bosons}^2(v_2)}{\partial v_2} W^\mu W_\mu + \frac{\partial m_{top}(v_2)}{\partial v_2} t\bar{t} + \frac{\partial M_{Higgs}^2(v_1, v_2)}{\partial v_2} = 0, \quad (26)$$

where W runs over all gauge fields.

If $M_{Higgs}^2(v_1, v_2)$ is like Eq. (13), in which there are no mixing terms of VEVs, this term can be separated into two terms such that each of the new terms only depends on one VEV. However, the fifth Higgs particles' masses in the 2HDM all have mixing terms.

Next, there are an important observation, that when the universe was cooling down to the value of v_2 after the big bang, the field Φ_2 broke the electroweak symmetry, and after that when the universe continued to cool down to the value of v_1 , the field Φ_1 continued to break the electroweak symmetry once again. The process of this electroweak symmetry breaking must be sequential. Hence, we cannot combine the two stages to study.

Therefore the rules for generating the masses of the particles through two symmetry breakings as follows:

Remark 1: At stage 1, Φ_2 breaks the symmetry or $v_2 \neq 0$, but now Φ_1 has not yet broken the symmetry so v_1 is still equal to 0. Hence, all the Higgs particles' masses only contain v_2 .

Remark 2: When the breaking symmetry occurs at Φ_1 , the interactions between Φ_2 and Φ_1 are turned on and v_1 would not be 0. In this stage, the further generated masses can not only depend on v_2 , but also on v_1 and the mixing of v_2 and v_1 .

Remark 3: With the above two remarks, through the mixing terms in the masses of the Higgs particles, the effects of the first stage has on the second stage. But they also make it difficult for investigating the phase transition at the later stage.

Remark 4: In order to view the two phase transition stages with the separated effective potentials, we can apply the following approximation to the mixing terms: $v_1.v_2 \sim \kappa.v_1^2$. Since at this time, v_2 can still change as the temperature decreases, it can consider the change of v_2 is now equal to κv_1 . This remark is actually a mathematical treatment like the approximation $v^2 = v_1^2 + v_2^2$. But when it is combined with the above third remarks, they make physical sense in the analysis of EWPT.

Therefore, from four remarks, all the Higgs particles' masses can be split into two different components,

$$M_{Higgs}^2(v_1, v_2) = m_{Higgs}^2(v_1) + m_{Higgs}^2(v_2). \quad (27)$$

Also the squared masses of the gauge and Higgs particles all can be split into two separate components at the tree level. From Eqs. (25) and (26), averaging over space and using Bose-Einstein and Fermi-Dirac distributions respectively for bosons and fermions to average over space, the one-loop effective potential can be obtained at high temperatures. Also according

to the analysis of Appendix A, the analysis of the Lagrangian of 2HDM into two separate components (as shown in Secs. II A, II B, II C), the total effective potential in the 2HDM model can be rewritten as

$$V_{eff}^{2HDM} = V_{eff}^{2HDM}(v_1) + V_{eff}^{2HDM}(v_2). \quad (28)$$

For further clarity, we restate the calculating process of the effective potential from the contributions of one-loop diagrams. The process of calculating the one-loop effective potential is the process of calculating the contribution of 1-loop diagrams with n external lines that are Higgs scalar fields (fields that act as mass generators). In the 2HDM, there are two Higgs fields (h, H) that act as such, corresponding to two VEVs (v_1, v_2). One-loop diagrams are shown in Figs. 1, 2, 3, 4.

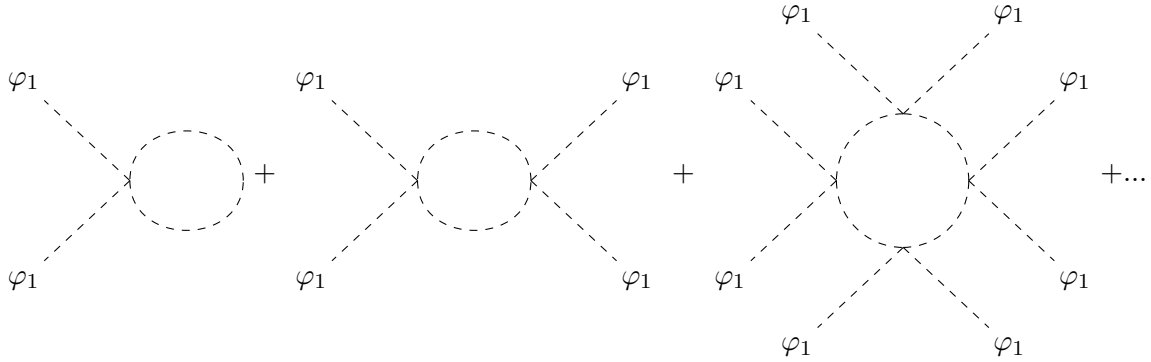


FIG. 1: The 1-loop contributions of the scalar fields

Similarly, also having diagrams where the external lines are φ_2 . The mixing $\varphi_1 - \varphi_2$ diagrams as Fig. 4.

In the above diagrams, φ_1 and φ_2 correspond to the terms of Higgs fields that only contain v_1 or v_2 . Since the 2HDM consists of two VEVs, having the mixing diagrams as in Fig. 4.

For the ϕ^4 theory, calculating the contributions of the diagrams as in Figs. 1, 2 and 3 is really easy, and this has been shown in Ref. [91]. However, the difficulty is to calculate the contributions of the diagrams in Fig. 4. As in Appendix A, we explicitly study the first diagram in Fig. 4 that translates to the following expression:

$$\Gamma_n(v_1, v_2) = i \frac{1}{2n} \int \frac{d^4 p}{(2\pi)^4} \left(\frac{i}{p^2 - m^2(v_1, v_2) + i\varepsilon} \right)^n (-i2\lambda_1)^{n_1/2} v_1^{n_1} (-i2\lambda_2)^{n_2/2} v_2^{n_2}, \quad (29)$$

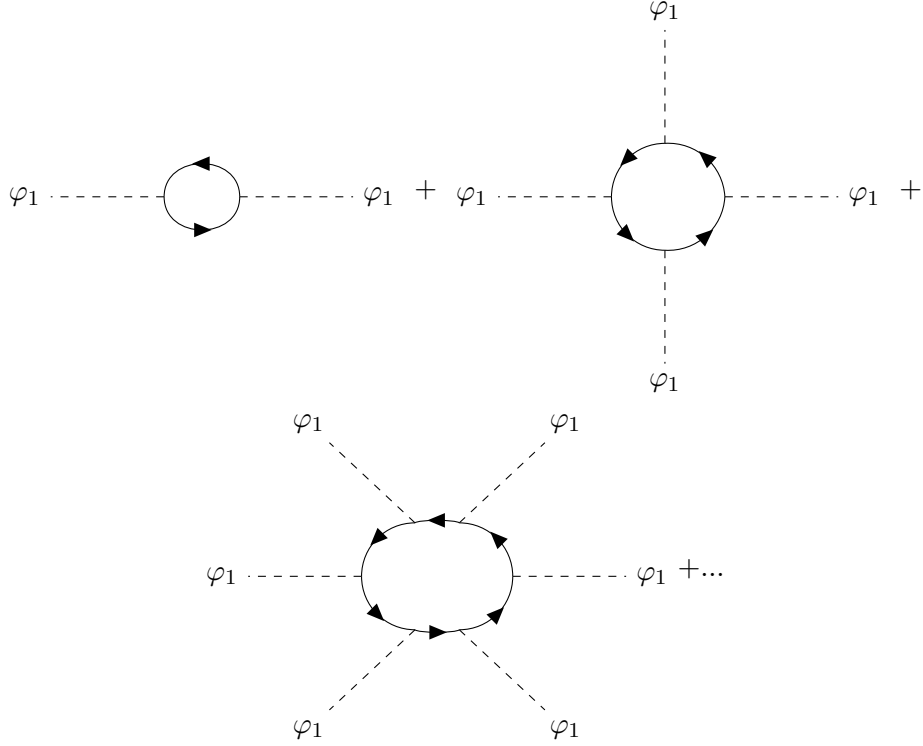


FIG. 2: The 1-loop contributions of the fermion fields

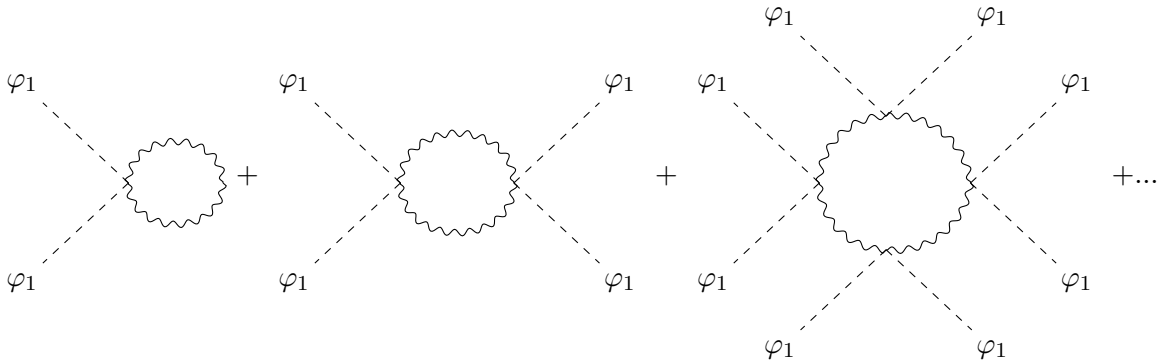


FIG. 3: The 1-loop contributions of the gauge fields

with $n_1 + n_2 = 2n$. Summing over all Γ_n with n runs from 0 to infinity, and hence n_1 and n_2 will also run from 0 to infinity. Hence calculating the integrals Γ_n and the infinite sums are very tricky. Since for each value of n , there are a sum that runs with n_1 or n_2 .

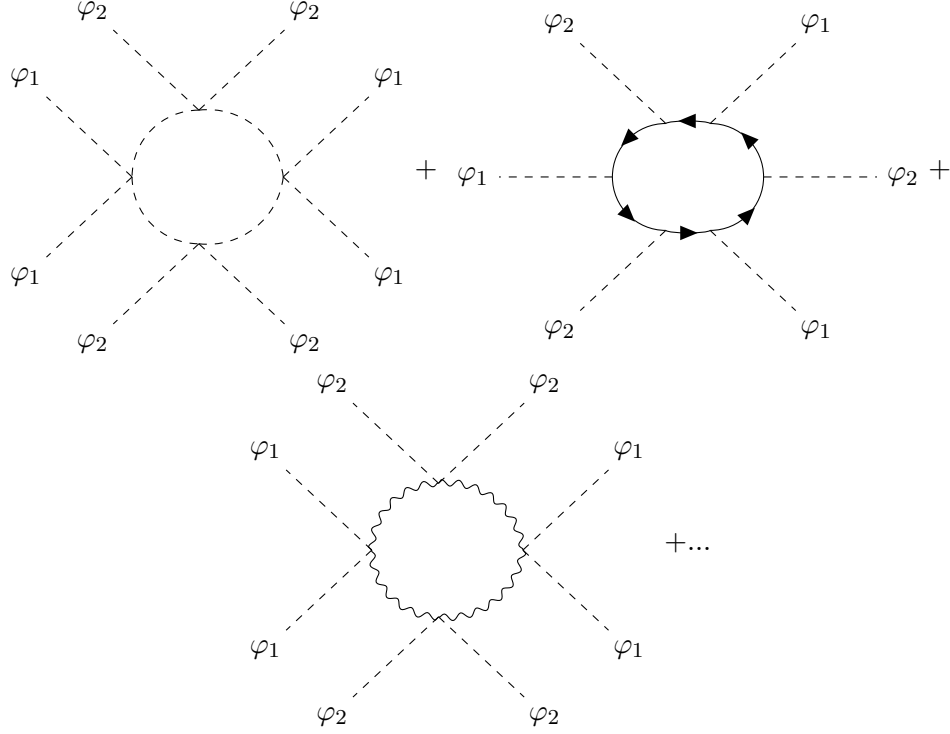


FIG. 4: The diagrams of one-loop contribution when there is a mix of $v_1 - v_2$

To quickly calculate Γ_n , from remarks 2 and 4, $\Gamma_n(v_1, v_2) \equiv \Gamma_n(v_1)$,

$$\Gamma_n(v_1, v_2) = i \frac{1}{2n} \int \frac{d^4 p}{(2\pi)^4} \left(\frac{i}{p^2 - m^2(v_1) + i\varepsilon} \right)^n v_1^{n_1} v_1^{n_2} \kappa^{n_2} (-i2\lambda_1)^{n_1/2} (-i2\lambda_2)^{n_2/2} \quad (30)$$

$$= i \frac{1}{2n} \int \frac{d^4 p}{(2\pi)^4} \left(-i2\lambda'_n \frac{i}{p^2 - m^2(v_1) + i\varepsilon} \right)^n v_1^{2n}. \quad (31)$$

Here, λ'_n must have some very small values in order for the series to converge. Therefore $\lambda'_n \sim \lambda'$. Hence, $\Gamma_n(v_1, v_2) \equiv \Gamma_n(v_1)$,

$$\Gamma_n(v_1) = i \frac{1}{2n} \int \frac{d^4 p}{(2\pi)^4} \left(2\lambda' \frac{v_1^2}{p^2 - m^2(v_1) + i\varepsilon} \right)^n. \quad (32)$$

Therefore the contributions from these mixing diagrams can be combined into the contribution from the diagrams that the external lines are just all φ_1 . In other words, by calculating the contributions from the diagrams, and applying Remarks 2, and 4, the mixing diagrams can be processed to turn the effective potential into two clearly separated components, one depends only on v_1 , while the other depends only on v_2 . In other words, the effective potential will be expressed as Eq. (28).

In the previous studies, to overcome the difficulties of dealing with the mixing terms of VEVs and to investigate the process of electroweak symmetry breaking similar to the SM,

the authors have converted v_1 and v_2 to v through $\tan\beta$ [55, 90]. This is a very clever technique, but in terms of physics, it needs to be interpreted with care. Since $v_1 \neq v_2$, the symmetry-breaking stages must be sequential. The fact that we write the same effective potential for v (shortly denoted as $V_{eff}(v)$) to calculate the strength of phase transition is not wrong, but we should only write it when $v_1 \ll v_2$, to clearly show the nature of the physics in the 2HDM. The limitations and utilities of this technique will be analyzed in the following sections where investigating the 2HDM- S_3 .

E. Comments on EWPT in the 2HDM

First, we have summarized of experimental as well as theoretical calculations leading to parameter regions in 2HDM models:

- Since the 125 GeV Higgs boson observed at the LHC, the model becomes consistent with the LHC Higgs data when the model provides such a Higgs particle [76]. $1 < \tan\beta$ can be precisely determined from the requirement of the light mass of the up- and down-quarks [76]. From here also admit the scenario $\mu_1, \mu_2, l_1, l_2 \neq 0$ and having the soft-breaking potential. Also according to Ref. [77], the mass of the nonstandard particles are less than 1 TeV, $0.3 < \tan\beta < 17$.
- Some references used the data from decay channels in LHC and investigated the value range of $\tan\beta$. In Ref. [92], the authors removed the circumstance $\tan\beta < 1$ for four types of 2HDM. In Ref. [93], the authors saw that in the decay channel $pp \rightarrow W \rightarrow hH^\pm$, the scattering amplitude of that channel is lasting over the change of $\tan\beta$ in the range of $1 < \tan\beta < 10$.
- The FCNC structure exists in the model. It is therefore compatible with current experimental data on quarks [76, 94]. The mass of exotic particle below 190 or 300 GeV has been already excluded by the data from the LHC Run-II and the HL-LHC, the most of the parameter region would be explored [95]. Since having a significant amount of the $b\bar{b}$ branching ratios for the additional Higgs bosons [95].
- The model under consideration contains the pseudoscalar field A being attached subject for recent experimental study [96].

- Next, in general, there are four types of 2HDM models of Z_2 symmetry. Two of the four types were investigated in Ref. [97] and also with parameter domains consistent with the above conclusions.

The above conclusions lead to an instruction for surveying 2HDM- S_3 also with a parameter region, $1 \sim \tan \beta < 17$ and the masses of additional bosons must be larger than 200 GeV.

More importantly, the following comments about the EWPT in 2HDM models after the observation of the 125 GeV Higgs at LHC (2012 are in order):

- According to Ref. [98], with LHC data and decay channel $h^0 \rightarrow \gamma\gamma$, for a strong first order EWPT in 2HDM, $m_A > 400$ GeV, a mass hierarchy $m_{H^\pm} < m_H < m_A$ and $1 < \tan \beta < 10$. This does not define the upper bounds of the masses of the particles, but the lower bounds are about 400 GeV.
- In Ref. [99], when analyzing the inert 2HDM model, for $500 \text{ GeV} < m_H < \text{a few TeV}$, for a first order EWPT, boson H could be a candidate for dark matter.
- The authors in Ref. [100] performed a nonperturbation study of EWPT in 2HDM. To have a first order EWPT, the condition is $m_A > m_H + m_Z$. This suggests that the mass of additional Higgs bosons must be larger mass than one of SM-like Higgs boson.
- In Ref. [101], for a first order EWPT and combined with LHC data, the masses of additional Higgs bosons are typically 300 – 400 GeV. The triple Higgs boson coupling is predicted to be 35 – 55 % larger than the standard model value.
- In Ref. [97], analyzing decay channels $A, H, H^\pm \rightarrow tt, tb$, combining with HL-LHC signal and gravitational wave observations at LISA. The 2HDM model for a first order EWPT. It also shows that these decay channels can be key channels to authenticate the first order EWPT in 2HDM.
- In particular, in Ref. [97], Fig. 1 shows that the ratio between two phase transition strengths of the two model types is almost independent of $\tan \beta$. Different scenarios between the masses of the additional Higgs particles were analyzed in the EWPT problem, such as $m_{H^\pm} = m_A$ or $m_H = m_{H^\pm}$.

The summaries of the EWPT results in the 2HDM model are important indicators for the parameter space in the calculation of EWPT in the 2HDM- S_3 . It also shows the effect of the S_3 symmetry, which will be discussed in the following sections.

III. REVIEW ON THE 2HDM- S_3

A. Particle content

To solve with FCNC for the 2HDM, ones can realize by implement of S_3 symmetry [102]. The particle contents and their charge assignment are given in Table I.

Particle	Q_a	L_a	L_τ	u_{aR}	d_{iR}	e_{aR}	τ_R	Φ_1	Φ_2
$SU(2)_L$	2	2	2	1	1	1	1	2	2
$U(1)_Y$	$\frac{1}{6}$	$-\frac{1}{2}$	$-\frac{1}{2}$	$\frac{2}{3}$	$-\frac{1}{3}$	-1	-1	$\frac{1}{2}$	$\frac{1}{2}$
S_3	1	2	1	1'	1 or 1'	2	1 or 1'	1	1'

TABLE I: The particle contents and their charge assignment of the $SU(2)_L \times U(1)_Y \times S_3$ symmetry.

There are two kinds of representations for S_3 : real and complex; and it is easier to work with complex representation [103].

B. Higgs potential

The generic scalar potential of 2HDM- S_3 [87] can be written as

$$\begin{aligned}
V_H = & m_{11}^2 \Phi_1^2 + m_{22}^2 \Phi_2^2 - m_{12}^2 \Phi_1 \cdot \Phi_2 - (m_{12}^2)^* \Phi_2 \cdot \Phi_1 \\
& + \frac{\lambda_1}{2} \Phi_1^4 + \frac{\lambda_2}{2} \Phi_2^4 + \lambda_3 \Phi_1^2 \Phi_2^2 + \lambda_4 (\Phi_1 \cdot \Phi_2) (\Phi_2 \cdot \Phi_1) \\
& + \left[\frac{\lambda_5}{2} (\Phi_1 \cdot \Phi_2)^2 + (\lambda_6 \Phi_1^2 + \lambda_7 \Phi_2^2) (\Phi_1 \cdot \Phi_2) + \text{H. c.} \right],
\end{aligned} \tag{33}$$

where any couplings other than m_{12}^2 , λ_5 , λ_6 , and λ_7 are real. Using $v_1/\sqrt{2}$ and $v_2/\sqrt{2}$ to denote the VEVs, but ignore the factor $\sqrt{2}$ (however, it was still included in the calculations).

If choosing $\Phi \sim (\mathbf{1}, \mathbf{1}')$ to be the representations of S_3 , then all the odd terms only containing Φ_2 , such as $m_{12}^2 \Phi_1 \cdot \Phi_2$, $(m_{12}^2)^* \Phi_2 \cdot \Phi_1$ and $(\lambda_6 \Phi_1^2 + \lambda_7 \Phi_2^2) (\Phi_1 \cdot \Phi_2)$ must be terminated for

the Lagrangian to be invariant under the S_3 group transformation, since the representation $\mathbf{1}'$ changes the sign of the fields with odd permutation. In this case, getting a Z_2 symmetric potential, in which $m_{12}^2 = \lambda_6 = \lambda_7 = 0$.

In general, we can assume that $\Phi \sim s$, where s denotes either of the two alternatives $(\mathbf{1}, \mathbf{1})$ or $(\mathbf{1}, \mathbf{1}')$. Because the labels 1 and 2 were selected at random, the case $\Phi \sim (\mathbf{1}', \mathbf{1})$ is also included. For its simplicity, a complicated representation can be selected to work with. The most common Higgs potential of a S_3 doublet is of the following form where the two scalars $\Phi = (\phi_1, \phi_2)^T$ transform as a doublet in a *complex* representation [87]:

$$V_C = \mu_1^2(\phi_2^2 + \phi_1^2) + \frac{1}{2}l_1(\phi_2^2 + \phi_1^2)^2 + \frac{1}{2}l_2(\phi_2^2 - \phi_1^2)^2 \\ + l_3(\phi_1 \cdot \phi_2)(\phi_2 \cdot \phi_1). \quad (34)$$

Note that both complex and real representations provide the similar result given in (34) which coincides with generic one V_H in (33) for the conditions [87]

$$m_{11}^2 = m_{22}^2 \equiv \mu_1^2, m_{12}^2 = 0, \lambda_1 = \lambda_2, \lambda_5 = 0. \quad (35)$$

C. The soft breaking of S_3 group

To break S_3 softly, Ma and Melic [104] include a soft potential by hand to the full one, while still preserving the $\phi_1 \leftrightarrow \phi_2$ symmetry,

$$V_{\text{soft}} = -\mu_2^2 \left(\phi_1^\dagger \phi_2 + \phi_2^\dagger \phi_1 \right). \quad (36)$$

Soft breaking terms here mean that they violate the original symmetry in the Higgs potential or the Lagrangian. They are 'soft' because the couplings associated with those terms are small. Without the above mentioned term, we will face the trouble of massless pseudoscalar A . Realistically, there should be some breaking terms which will take care of this problem.

In a spontaneously broken case, you break the symmetry of the ground state and it naturally breaks the symmetry in the Lagrangian. On the other hand, in this case, those terms must be added by hand to break the symmetry. The potential then becomes $V_C + V_{\text{soft}}$.

The term containing V_{soft} makes the mass of the pseudoscalar Higgs particle A always nonzero in all cases. If there is no V_{soft} term, the Higgs particle A will have a mass of 0, when $v_1 = v_2$. Besides, the term V_{soft} must exist, since it represents the direct interaction

between ϕ_1 and ϕ_2 . Therefore, we must study the Higgs potential that contains the term V_{soft} .

IV. ELECTROWEAK PHASE TRANSITION IN THE 2HDM- S_3

A. A vital role of S_3

First, the function of the S_3 group in the 2HDM- S_3 can be shown by comparing the Higgs potential of the two models before and after adding S_3 symmetry. Let us consider the Higgs potential of 2HDM which has the following form

$$V_{\text{Higgs}}^{2\text{HDM}} = m_{11}^2 \Phi_1^\dagger \Phi_1 + m_{22}^2 \Phi_2^\dagger \Phi_2 - m_{12}^2 (\Phi_1^\dagger \Phi_2 + \Phi_2^\dagger \Phi_1) + \frac{\lambda_1}{2} (\Phi_1^\dagger \Phi_1)^2 + \frac{\lambda_2}{2} (\Phi_2^\dagger \Phi_2)^2 + \lambda_3 \Phi_1^\dagger \Phi_1 \Phi_1^\dagger \Phi_2 + \lambda_4 \Phi_1^\dagger \Phi_2 \Phi_2^\dagger \Phi_1 + \frac{\lambda_5}{2} \left[(\Phi_1^\dagger \Phi_1)^2 + (\Phi_2^\dagger \Phi_2)^2 \right]. \quad (37)$$

The above Higgs potential contains 8 parameters, and the squared masses of Higgs particles are given by

$$\begin{aligned} m_{H^\pm, 2HDM}^2 &= \left(\frac{m_{12}^2}{v_1 v_2} - \lambda_4 - \lambda_5 \right) v^2, \\ m_{A, 2HDM}^2 &= \left(\frac{m_{12}^2}{v_1 v_2} - 2\lambda_5 \right) (v_1^2 + v_2^2), \\ m_{h, 2HDM}^2 &= \frac{1}{2} \left[(\lambda_1 v_1^2 + \lambda_2 v_2^2) + m_{12}^2 \frac{v^2}{v_1 v_2} \right] \\ &\quad - \sqrt{\left[\frac{\lambda_1 v_1^2 - \lambda_2 v_2^2}{2} - \frac{m_{12}^2}{2v_1 v_2} (v_1^2 - v_2^2) \right]^2 + (\lambda_{345} v_1 v_2 - m_{12}^2)^2}, \\ m_{H, 2HDM}^2 &= \frac{1}{2} \left[(\lambda_1 v_1^2 + \lambda_2 v_2^2) + m_{12}^2 \frac{v^2}{v_1 v_2} \right] \\ &\quad + \sqrt{\left[\frac{\lambda_1 v_1^2 - \lambda_2 v_2^2}{2} - \frac{m_{12}^2}{2v_1 v_2} (v_1^2 - v_2^2) \right]^2 + (\lambda_{345} v_1 v_2 - m_{12}^2)^2}. \end{aligned} \quad (38)$$

Looking at the formulas of masses in (38), we see that they contain the very annoying mixing terms of v_1 and v_2 . Hence, at nonzero temperatures, these mixing terms make the job of calculating the contributions from the particles to the effective potential very difficult. They turn the symmetry breaking process into the process of breaking the ambiguous mixings of Φ_1 and Φ_2 .

Meanwhile, in the complex representation, the Higgs potential of 2HDM- S_3 has a simpler

form:

$$\begin{aligned}
V_{\text{Higgs}}^{2\text{HDM}\otimes S_3} &\equiv V(\phi_1, \phi_2) \\
&= \mu_1^2(\phi_2^2 + \phi_1^2) + \frac{1}{2}l_1(\phi_2^2 + \phi_1^2)^2 + \frac{1}{2}l_2(\phi_2^2 - \phi_1^2)^2 \\
&\quad + l_3(\phi_1 \cdot \phi_2)(\phi_2 \cdot \phi_1) - \mu_2^2(\phi_1 \cdot \phi_2 + \phi_2 \cdot \phi_1).
\end{aligned} \tag{39}$$

Seeing the structure of those Higgs potentials containing S_3 symmetry, ones conclude that the Higgs potential becomes simpler, with fewer parameters (from 8 reduced to 5). Thanks to that, the forms of Higgs mass are also simpler. By replacing v_1 and v_2 by $c_\beta v$ and $s_\beta v$, in expressions of H and h masses, ones get a form of v -dependent.

$$\begin{aligned}
m_{H^\pm, S_3}^2 &= -l_2 v^2, \\
m_{A, S_3}^2 &= -\frac{1}{2}(2l_2 - l_3)v^2, \\
m_{H, S_3}^2 &= \frac{1}{4}v^2 \left[2l_1 + l_3 + \sqrt{16l_1 l_2 (c_\beta^2 - s_\beta^2)^2 - 8l_2 l_3 + l_3^2 - 4l_1 l_3 (c_\beta^4 - 6c_\beta^2 s_\beta^2 + s_\beta^4)} \right] = \frac{1}{4}f_H \cdot v^2, \\
m_{h, S_3}^2 &= \frac{1}{4}v^2 \left[2l_1 + l_3 - \sqrt{16l_1 l_2 (c_\beta^2 - s_\beta^2)^2 - 8l_2 l_3 + l_3^2 - 4l_1 l_3 (c_\beta^4 - 6c_\beta^2 s_\beta^2 + s_\beta^4)} \right] = \frac{1}{4}f_h \cdot v^2.
\end{aligned} \tag{40}$$

The S_3 symmetry has removed the mixing parts of the two VEVs inside the mass of two charged Higgs bosons H^\pm and one neutral Higgs boson A . Otherwise, h and H still have the mixing parts hiding in c_β and s_β . However, this mixing would be simpler in the 2HDM, since there are no such ratios as v_1/v_2 or $v^2/(v_1 \cdot v_2)$, their mass formulas then have fewer parameters and are simpler than the ones of 2HDM without S_3 .

Therefore, according to the remarks for the 2HDM, S_3 had made the process of the electroweak phase transition occur in each VEV. This will be discussed in the next section.

B. Structure of EWPT

The procedure to describe the structure of electroweak phase transition in this model is similar to that in the SM, whereas Higgs and gauge bosons are the main contributors in the breaking symmetry process. For that reason, determination mass can also affect the phase transition.

The 2HDM with S_3 symmetry has Higgs Lagrangian with kinetic and potential elements

as

$$\mathcal{L}_{\text{Higgs}} = (D_\mu \phi_1)^\dagger (D^\mu \phi_1) + (D_\mu \phi_2)^\dagger (D^\mu \phi_2) - V(\phi_1, \phi_2). \quad (41)$$

Averaging all over the space, then replacing fields with VEVs, the Higgs Lagrangian with variables v_1 and v_2 (with $v_1 \neq v_2$) has the following form:

$$\mathcal{L}_{\text{Higgs}} = \frac{1}{2} \partial^\mu v_1 \partial_\mu v_1 + \frac{1}{2} \partial^\mu v_2 \partial_\mu v_2 - V_0(v_1, v_2) + \sum_{i=\text{vector boson}} m_i^2(v_1, v_2) W^\mu W_\mu + \sum_{j=\text{Higgs boson}} m_j^2(v_1, v_2) H^2, \quad (42)$$

whereas W and H are the vector boson and scalar fields, respectively.

Table II contains the squared mass of the particles contributing to the EWPT, in the form of depending VEVs; n is the degree of freedom of the fields. The masses of known particles are in generic form and at 0K, shown in Table III.

Particles	$m^2(v_1, v_2)$	$m^2(v_1)$	$m^2(v_2)$	n
$m_{W^\pm}^2$	$\frac{g^2 v^2}{4}$	$\frac{g^2 v_1^2}{4}$	$\frac{g^2 v_2^2}{4}$	6
m_Z^2	$(g^2 + g'^2) \frac{v^2}{4}$	$(g^2 + g'^2) \frac{v_1^2}{4}$	$(g^2 + g'^2) \frac{v_2^2}{4}$	3
m_h^2	$\frac{1}{4} f_h v^2$	$\frac{1}{4} f_h v_1^2$	$\frac{1}{4} f_h v_2^2$	1
m_H^2	$\frac{1}{4} f_H v^2$	$\frac{1}{4} f_H v_1^2$	$\frac{1}{4} f_H v_2^2$	1
m_A^2	$-\frac{1}{2}(2l_2 - l_3)v^2$	$-\frac{1}{2}(2l_2 - l_3)v_1^2$	$-\frac{1}{2}(2l_2 - l_3)v_2^2$	1
$m_{H^\pm}^2$	$-l_2 v^2$	$-l_2 v_1^2$	$-l_2 v_2^2$	2
m_t^2	$f_t^2 v^2$	$f_t^2 v_1^2$	$f_t^2 v_2^2$	-12

TABLE II: Squared mass of the gauge bosons and scalar bosons in 2HDM- S_3 ; whereas mass of the W^\pm , Z and t is the same as the one in SM; $v^2 = v_1^2 + v_2^2$.

Particles	$m_{W^\pm}(v_0)$	$m_Z(v_0)$	$m_h(v_0)$	$m_t(v_0)$
$m(v_0)$ [GeV]	80.442	91.18	125	173.1

TABLE III: Mass of particles (GeV) at 0K in 2HDM- S_3

Table II shows us that all the particles in the model depend on two VEVs. But v_1 and v_2 depend on each other, $v_2/v_1 = \tan \beta$. The forms of mass could be changed into

one-VEV-depended ($v = \sqrt{v_1^2 + v_2^2}$) by replacing $v_1 = vc_\beta$ and $v_2 = vs_\beta$. Therefore, in this model, assuming the remark 4, the electroweak phase transition can be considered as a dual transition, with two VEVs accomplished to the condition $v = \sqrt{v_1^2 + v_2^2}$ and at 0K, $v_0 = \sqrt{v_{01}^2 + v_{02}^2} = 246$ GeV.

Here in remark 4, it is also a note that the coefficient κ is now equal to $\tan\beta$. Carefully observing Table II, although the masses of h and H can be split, there still exists the coefficient κ in f_h and f_H . These constants are only meaningful in that the masses of h and H can be split into terms that each one of them depends only on one VEV. In other words, the contributions of the mixing of v_1 and v_2 are all brought back to only one VEV is v_1 or v_2 , and the difference between v_1 and v_2 is put into the constants f_h and f_H . Hence, the investigation of phase transition is somewhat relatively easier. But in the end, the replacement is really not that important, since in the next sections, this coefficient in fact will not have any effects on the strength of phase transition.

C. The effective potential

This dual-phase transition has the participation of new particles as two charged Higgs H^\pm , one neutral CP -odd A , and one neutral CP -even H . More importantly, there are also the presence of SM particles as one neutral CP -even Higgs boson h , two charged gauge bosons W^\pm , one neutral boson Z and top quark t .

The effective potential for each stage can be calculated in two ways. The effective potentials only contain the contributions from the particles outside of the SM and the gauge bosons, SM-like Higgs boson and top quark. The other particles have small values of mass so they can be just ignored. The process of calculating the effective potential is in detail given in Ref. [71].

The effective potential of one phase transition without daisy loops has the form:

$$\begin{aligned}
V_{eff}(\mathcal{V}, T) = & V_0(\mathcal{V}) + \frac{1}{64\pi^2} \left[6m_{W^\pm}^4(\mathcal{V}) \ln \frac{m_{W^\pm}^2(\mathcal{V})}{Q^2} + 3m_Z^4(\mathcal{V}) \ln \frac{m_Z^2(\mathcal{V})}{Q^2} + 2m_{H^\pm}^4(\mathcal{V}) \ln \frac{m_{H^\pm}^2(\mathcal{V})}{Q^2} \right. \\
& + m_h^4(\mathcal{V}) \ln \frac{m_h^2(\mathcal{V})}{Q^2} + m_H^4(\mathcal{V}) \ln \frac{m_H^2(\mathcal{V})}{Q^2} + m_A^4(\mathcal{V}) \ln \frac{m_A^2(\mathcal{V})}{Q^2} - 12m_t^4(\mathcal{V}) \ln \frac{m_t^2(\mathcal{V})}{Q^2} \Big] \\
& + \frac{T^4}{4\pi^2} \left[6F_- \left(\frac{m_{W^\pm}(\mathcal{V})}{T} \right) + 3F_- \left(\frac{m_Z(\mathcal{V})}{T} \right) + 2F_- \left(\frac{m_{H^\pm}(\mathcal{V})}{T} \right) + F_- \left(\frac{m_h(\mathcal{V})}{T} \right) \right. \\
& \left. + F_- \left(\frac{m_H(\mathcal{V})}{T} \right) + F_- \left(\frac{m_A(\mathcal{V})}{T} \right) + 12F_+ \left(\frac{m_t(\mathcal{V})}{T} \right) \right],
\end{aligned} \tag{43}$$

whereas

$$F_\pm \left(\frac{m_\phi}{T} \right) = \int_0^{\frac{m_\phi}{T}} \alpha J_\pm^{(1)}(\alpha, 0) d\alpha, \tag{44}$$

$$J_\pm^{(1)}(\alpha, 0) = 2 \int_\alpha^\infty \frac{(x^2 - \alpha^2)^{\nu/2}}{e^x \pm 1} dx. \tag{45}$$

Then,

$$\begin{cases} J_-^{(1)}(\alpha, 0) = \frac{\pi^2}{3} - \pi\alpha - \frac{\alpha^2}{2} \left(\ln \frac{\alpha}{4\pi} + C - \frac{1}{2} \right) + \mathcal{O}(\alpha^2), \\ J_+^{(1)}(\alpha, 0) = \frac{\pi^2}{6} - \frac{\alpha^2}{2} \left(\ln \frac{\alpha}{\pi} + C - \frac{1}{2} \right) + \mathcal{O}(\alpha^2). \end{cases} \tag{46}$$

This process has the contribution from five Higgs particles in total into the effective potential. However, there are only two scalar Higgs particles h, H , which are associated with the two nonzero vacuum expectation values v_1, v_2 . Therefore, the minimum conditions then are

$$V_{eff}(\mathcal{V}_0, 0) = 0, \quad \left. \frac{\partial V_{eff}(\mathcal{V}, 0)}{\partial \mathcal{V}} \right|_{\mathcal{V}=\mathcal{V}_0} = 0, \tag{47}$$

$$\left. \frac{\partial^2 V_{eff}(\mathcal{V}, 0)}{\partial \mathcal{V}^2} \right|_{\mathcal{V}=\mathcal{V}_0} = [m_h^2(\mathcal{V}) + m_H^2(\mathcal{V})]_{\mathcal{V}=\mathcal{V}_0}. \tag{48}$$

With the minimum conditions, expanding the functions of J_\pm , the effective potential can be rewritten as

$$V_{eff}(\mathcal{V}) = \frac{\lambda_T}{4} \mathcal{V}^4 - \theta T \mathcal{V}^3 + \gamma (T^2 - T_0^2) \mathcal{V}^2, \tag{49}$$

where,

$$\begin{aligned}
\lambda_T &= \frac{m_h^2(\mathcal{V}_0) + m_H^2(\mathcal{V}_0)}{2\mathcal{V}_0^2} \left\{ 1 + \frac{1}{8\pi^2\mathcal{V}_0^2 [m_h^2(\mathcal{V}_0) + m_H^2(\mathcal{V}_0)]} \times \right. \\
&\quad \left[6m_{W^\pm}^4(\mathcal{V}_0) \ln \frac{bT^2}{m_{W^\pm}^2(\mathcal{V}_0)} + 3m_Z^4(\mathcal{V}_0) \ln \frac{bT^2}{m_Z^2(\mathcal{V}_0)} + 2m_{H^\pm}^4(\mathcal{V}_0) \ln \frac{bT^2}{m_{H^\pm}^2(\mathcal{V}_0)} \right. \\
&\quad \left. + m_h^4(\mathcal{V}_0) \ln \frac{bT^2}{m_h^2(\mathcal{V}_0)} + m_H^4(\mathcal{V}_0) \ln \frac{bT^2}{m_H^2(\mathcal{V}_0)} + m_A^4(\mathcal{V}_0) \ln \frac{bT^2}{m_A^2(\mathcal{V}_0)} - 12m_t^4(\mathcal{V}_0) \ln \frac{b_F T^2}{m_t^2(\mathcal{V}_0)} \right] \Big\}, \\
\theta &= \frac{1}{12\pi\mathcal{V}_0^3} \left[6m_{W^\pm}^3(\mathcal{V}_0) + 3m_Z^3(\mathcal{V}_0) + 2m_{H^\pm}^3(\mathcal{V}_0) + m_h^3(\mathcal{V}_0) + m_H^3(\mathcal{V}_0) + m_A^3(\mathcal{V}_0) \right], \\
\gamma &= \frac{1}{24\mathcal{V}_0^2} \left[6m_{W^\pm}^2(\mathcal{V}_0) + 3m_Z^2(\mathcal{V}_0) + 2m_{H^\pm}^2(\mathcal{V}_0) + m_h^2(\mathcal{V}_0) + m_H^2(\mathcal{V}_0) + m_A^2(\mathcal{V}_0) + 6m_t^2(\mathcal{V}_0) \right], \\
T_0^2 &= \frac{1}{4\gamma} \left\{ m_h^2(\mathcal{V}_0) + m_H^2(\mathcal{V}_0) - \frac{1}{8\pi^2\mathcal{V}_0^2} \left[6m_{W^\pm}^4(\mathcal{V}_0) + 3m_Z^4(\mathcal{V}_0) + 2m_{H^\pm}^4(\mathcal{V}_0) \right. \right. \\
&\quad \left. \left. + m_h^4(\mathcal{V}_0) + m_H^4(\mathcal{V}_0) + m_A^4(\mathcal{V}_0) - 12m_t^4(\mathcal{V}_0) \right] \right\}.
\end{aligned} \tag{50}$$

The critical temperature T_c is given by

$$T_c = \frac{T_0}{\sqrt{1 - \theta^2/[\gamma\lambda_{T_c}]}} \tag{51}$$

and the critical VEV can be derived as

$$\mathcal{V}_c = \frac{2\theta T_c}{\lambda_{T_c}}. \tag{52}$$

Therefore, the strength of EWPT is

$$S = \frac{\mathcal{V}_c}{T_c} = \frac{2\theta}{\lambda_{T_c}}. \tag{53}$$

Next, taking into account daisy loops, the effective potential will have the form:

$$V_{eff}^{daisy} = V_{eff}(\mathcal{V}) - V^d(\mathcal{V}), \tag{54}$$

in which the second component on the right-hand side of Eq. (54) is the contribution of daisy loops [105–107] (especially the appendix A in Ref. [107]). Here, degrees of freedom are given by: $g_Z = 3, g_W = 6, g_h = g_A = g_H = 1, g_{H^\pm} = 2$ and

$$V^d(\mathcal{V}) = \frac{T}{12\pi} \sum_{i=h,W,Z,A,H,H^\pm} g_i \left\{ \left[\frac{m_i^2(\mathcal{V}_0)\mathcal{V}^2}{\mathcal{V}_0^2} + \Pi_i(T) \right]^{3/2} - \frac{m_i^3(\mathcal{V}_0)\mathcal{V}^3}{\mathcal{V}_0^3} \right\}, \tag{55}$$

$$\begin{aligned}
\Pi_W(T) &= \frac{22}{3} \frac{m_W^2(\mathcal{V}_0)}{\mathcal{V}_0^2} T^2, \\
\Pi_Z(T) &= \frac{22}{3} \frac{(m_Z^2(\mathcal{V}_0) - m_W^2(\mathcal{V}_0))}{\mathcal{V}_0^2} T^2, \\
\Pi_h(T) &= \frac{2m_W^2(\mathcal{V}_0) + m_Z^2(\mathcal{V}_0) + m_h^2(\mathcal{V}_0) + 2m_t^2(\mathcal{V}_0)}{4\mathcal{V}_0^2} T^2 + (\Lambda_{hH} + \Lambda_{hA} + \Lambda_{hH^\pm}).T^2. \quad (56)
\end{aligned}$$

As for exotic Higgs particles then

$$\Pi_{h-exotic} = (\Lambda_{hH} + \Lambda_{hA} + \Lambda_{hH^\pm}).T^2 \quad (57)$$

$$\begin{aligned}
\Pi_A(T) &\sim \frac{m_A^2(\mathcal{V}_0)}{\mathcal{V}_0^2} T^2, \\
\Pi_H(T) &\sim \frac{m_H^2(\mathcal{V}_0)}{\mathcal{V}_0^2} T^2, \\
\Pi_{H^\pm}(T) &\sim \frac{m_{H^\pm}^2(\mathcal{V}_0)}{\mathcal{V}_0^2} T^2. \quad (58)
\end{aligned}$$

$\Lambda_{hH} + \Lambda_{hA} + \Lambda_{hH^\pm}$ are coefficients representing the contribution from exotic Higgs daisy loops to SM-like Higgs boson. A , H , H^\pm are called exotic Higgs for short.

The daisy loops of exotic Higgs boson can be omitted, since these masses of particles are large and $m(\mathcal{V})/T \sim 1$ [105]. This can be explained in Sec. IV F.

Note that \mathcal{V} can be v_1, v_2 or v . Let $v^2 = a.v_2^2$, the relation between $\tan \beta$ and a is

$$\tan \beta = \sqrt{1/(a-1)}. \quad (59)$$

From this, the masses of the particles in terms of a are given in Table IV.

Particles	$m^2(v_1, v_2)$	$m^2(v_2)$	$m^2(v_1)$
$m_{W^\pm}^2$	$\frac{g^2 v^2}{4}$	$m_{W^\pm}^2/a$	$m_{W^\pm}^2(v_2).(a-1)$
m_Z^2	$(g^2 + g'^2) \frac{v^2}{4}$	m_Z^2/a	$m_Z^2(v_2).(a-1)$
m_h^2	$\frac{1}{4} f_h v^2$	m_h^2/a	$m_h^2(v_2).(a-1)$
m_H^2	$\frac{1}{4} f_H v^2$	m_H^2/a	$m_H^2(v_2).(a-1)$
m_A^2	$-\frac{1}{2}(2l_2 - l_3)v^2$	m_A^2/a	$m_A^2(v_2).(a-1)$
$m_{H^\pm}^2$	$-l_2 v^2$	$m_{H^\pm}^2/a$	$m_{H^\pm}^2(v_2).(a-1)$
m_t^2	$f_t^2 v^2$	m_t^2/a	$m_t^2(v_2).(a-1)$

TABLE IV: Squared mass of the gauge bosons and scalar bosons in 2HDM- S_3 .

With v_1 different from v_2 , this model has two stages of phase transition. We assume that $v_1 < v_2$, which means $1 < a < 2$ or $1 < \tan \beta$. As the above sections pointed out, in 2HDM- S_3 , the particles' masses can be changed such that there are no mixing terms between v_1 and v_2 . So the correct effective potential for this model is

$$V_{eff}^{S_3} = V_{eff}^{S_3}(v_1) + V_{eff}^{S_3}(v_2). \quad (60)$$

With the above formula for the potential, the phase transition's strength does not depend on a .

D. Probing the independence of EWPT strength on $\tan \beta$

Note that the EWPT in this model occurs in two stages and the mass components of the involved particles are given in Table IV. Let us assume that the phase transition's strength of the first stage has already been calculated, $S_1 > 1$ for $\mathcal{V} = v_2$.

It would like to prove that the second phase transition's strength (S_2), corresponds to $\mathcal{V}^2 = v_1^2 = v_2^2(a-1)$ will actually not change, that it is still equal to S_1 . Or in other words, it does not depend on a .

To do this, the functions $\lambda_{T_c}(v_1), \theta(v_1), \gamma(v_1), T_c(v_1)$ must be indicated the independent of a (equal to themselves when calculated with v_2). First, let us consider the function θ correspond to $\mathcal{V} = v_1$,

$$\theta(v_1) = \frac{1}{12\pi v_1^3} \left[6m_{W^\pm}^3(v_1) + 3m_Z^3(v_1) + 2m_{H^\pm}^3(v_1) + m_h^3(v_1) + m_H^3(v_1) + m_A^3(v_1) \right]. \quad (61)$$

The masses in the bracket and v_1 all have the same power of 3. Hence they are all proportional to $(a-1)^{3/2}$. By extracting this factor out of the masses and canceling it with the exact same factor from v_1 in the denominator, $\theta(v_1)$ is independent of a , or $\theta(v_1) = \theta(v_2)$. Similarly $\gamma(v_1)$ does not depend on a , but $T_0^2(v_1)$ depends on $(a-1)$, specifically $T_0^2(v_1) = (a-1)T_0^2(v_2)$. Because of this dependence on $(a-1)$ of $T_0^2(v_1)$, $\lambda_{T_c}(v_1)$ will not depend on a . The proof is

as follows. Consider the function λ_{T_c} corresponds to v_1 ,

$$\begin{aligned} \lambda_{T_c}(v_1) = & \frac{m_h^2(v_1) + m_H^2(v_1)}{2v_1^2} \left\{ 1 + \frac{1}{8\pi^2 v_1^2 [m_h^2(v_1) + m_H^2(v_1)]} \times \right. \\ & \left[6m_{W^\pm}^4(v_1) \ln \frac{bT_c^2(v_1)}{m_{W^\pm}^2(v_1)} + 3m_Z^4(v_1) \ln \frac{bT_c^2(v_1)}{m_Z^2(v_1)} + 2m_{H^\pm}^4(v_1) \ln \frac{bT_c^2(v_1)}{m_{H^\pm}^2(v_1)} \right. \\ & + m_h^4(v_1) \ln \frac{bT_c^2(v_1)}{m_h^2(v_1)} + m_H^4(v_1) \ln \frac{bT_c^2(v_1)}{m_H^2(v_1)} + m_A^4(v_1) \ln \frac{bT_c^2(v_1)}{m_A^2(v_1)} \\ & \left. \left. - 12m_t^4(v_1) \ln \frac{b_F T_c^2(v_1)}{m_t^2(v_1)} \right] \right\}. \end{aligned} \quad (62)$$

With T_c is given by Eq. (51) in the no daisy loop case. By the same reasoning from above, $\lambda_{T_c}(v_1)$ will not depend on a when the logarithmic factors do not depend on a . Indeed, we consider the general expression inside the logarithmic functions:

$$\begin{aligned} \frac{T_c^2(v_1)}{m^2(v_1)} &= \frac{T_0^2(v_1)}{[1 - \theta^2(v_1)/\gamma(v_1)\lambda_{T_c}(v_1)] m^2(v_2)} \\ &= \frac{(a-1)T_0^2(v_2)}{(1 - \theta^2(v_2)/\gamma(v_2)\lambda_{T_c}(v_1)) (a-1)m^2(v_2)} \\ &= \frac{T_0^2(v_2)}{(1 - \theta^2(v_2)/\gamma(v_2)\lambda_{T_c}(v_1)) m^2(v_2)}, \end{aligned} \quad (63)$$

in which the functions $\theta(v_1), \gamma(v_1)$ are all independent of a as proven earlier. The expression inside the logarithmic functions actually depends on $\lambda_{T_c}(v_1)$. Substitute the expression Eq. (63) into Eq. (62), we can finally realize that a no longer appears in the expression Eq. (62). This proves that $\lambda_{T_c}(v_1)$ does not depend on a . So, the functions $\lambda_{T_c}(v_1), \theta(v_1), \gamma(v_1), T_c(v_1)$ is truly independent of a when the effective potential without daisy loops.

When the effective potential with daisy loops which is Eq. (54), the critical temperature $T_C(v_1)$ is not Eq. (51) but $T_C(v_1) \sim T_0(v_1)$. So $\lambda_{T_C}(v_1)$ still does not depend on a . Furthermore, by the similar proof, $V^d(v_1)$ does not depend on a . Because $V^d(v_1)$ just depends on the ratio $m^2(\mathcal{V})/\mathcal{V}^2$. So finally at the critical temperature, the effective potential with daisy loops $[V_{eff}^{daisy-S_3}(v_1)]$ remains independent of a and deduced that S in the same regardless of being calculated with v_1 or v_2 .

This result agrees with the conclusions in Ref. [88], which concludes that $\tan \beta$ is not a meaningful parameter in the 2HDM.

Also commented in Sec. II E, in the Fig. 1 of Ref. [97], in the 2HDM model, since the ratio between the two phase transition strengths may not depend much on $\tan \beta$. In other

words, the strength of the phase transition can be independent of $\tan\beta$. We have clearly demonstrated this in the 2HDM- S_3 model, thanks to the S_3 symmetry that separates the two phase transitions.

E. The true critical temperatures

To indicate critical temperatures in the model, the effective potential without daisy loops is only used. The estimation of daisy loop contributions will be done in Sec. IV F. As analyzed in Sec. IV B, the 2HDM- S_3 model will have two critical temperatures which correspond to the two stages.

Since the coefficients are independent of a as shown above, the parameters of the second phase transition can be expressed in terms of the parameters of the first phase transition,

$$\lambda_{T,v_1} = \lambda_{T,v_2} = \lambda_{T,v}, \quad (64)$$

$$\theta_{v_1} = \theta_{v_2} = \theta_v, \quad (65)$$

$$\gamma_{v_1} = \gamma_{v_2} = \gamma_v, \quad (66)$$

$$T_{0,v_2}^2 = T_{0,v_1}^2 / (a - 1) = T_{0,v}^2 / a. \quad (67)$$

With these equalities, the effective potentials of the second stage and the combined stages can be expressed in terms of the effective potential of the first phase transition stage

$$V_{eff}^{S_3}(v_2) = \frac{\lambda_T}{4}v_2^4 - \theta T_{v_2}v_1^3 + \gamma(T_{v_1}^2 - T_{0,v_1}^2)v_1^2, \quad (68)$$

$$V_{eff}^{S_3}(v_1) = \frac{\lambda_T}{4}v_1^4 - \theta T_{v_1}v_1^3 + \gamma(T_{v_1}^2 - T_{0,v_1}^2)v_1^2 \quad (69)$$

$$= (a - 1)^2 \frac{\lambda_T}{4}v_2^4 - (a - 1)^2 \theta T_{v_2}v_2^3 + (a - 1)^2 \gamma(T_{v_2}^2 - T_{0,v_2}^2)v_2^2 \quad (70)$$

$$= (a - 1)^2 V_{eff}(v_2), \quad (71)$$

$$V_{eff}(v) = \frac{\lambda_T}{4}v^4 - \theta T_v v^3 + \gamma(T_v^2 - T_{0,v}^2)v^2 \quad (72)$$

$$= a^2 \frac{\lambda_T}{4}v_2^4 - a^2 \theta T_{v_2}v_2^3 + a^2 \gamma(T_{v_2}^2 - T_{0,v_2}^2)v_2^2 = a^2 V_{eff}(v_2). \quad (73)$$

Hence, $V_{eff}(v) \neq V_{eff}^{S_3}(v_1) + V_{eff}^{S_3}(v_2) = V_{eff}^{S_3}$. From these equations, $V_{eff}(v)$ can be deduced

$$V_{eff}(v) = \frac{a^2}{(a - 1)^2 + 1} V_{eff}^{S_3} = f(a) V_{eff}^{S_3}. \quad (74)$$

Here when writing down the effective potential of the system in terms of $V_{eff}(v)$, the correct effective potential of the system has been multiplied by $\frac{a^2}{(a-1)^2+1}$ times.

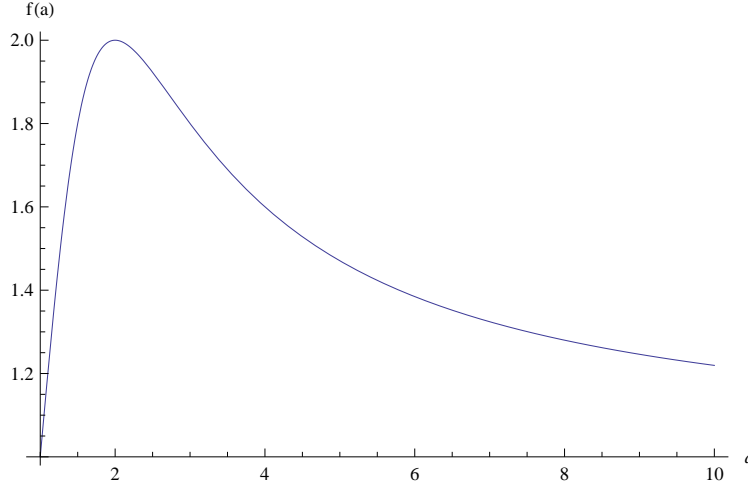


FIG. 5: The function $f(a)$, the ratio between $V_{eff}^{S_3}$ and $V_{eff}(v)$

According to Fig. 5, it follows $1 < a < 2$, and function $f(a)$ has value of 1 at $a = 1$, that is $V_{eff}(v) = V_{eff}^{S_3}$, or $v_1 = 0$, but this cannot be true. The maximum value of function $f(a)$ is 2 when $a = 2$, which is $v_1 = v_2$. Therefore when the two VEVs are equal to each other, the difference between the two effective potentials is at maximum. When $a > 2$ or $v_1 > v_2$, it can exchange $v_1 \longleftrightarrow v_2$, so that this case is similar to the case of $a < 2$.

When the effective potential is rewritten as $V_{eff}(v)$ when calculating the phase transition's strength, our S is correct. However, now the temperature of the phase transition T_C of the system turns out not to be correct. If $v_1 \neq v_2$, our system has two phase transition temperatures $T_{C1} < T_C$ and $T_{C2} < T_C$, respectively. Hence, writing down the effective potential for the system as $V_{eff}(v)$ is just a way to compare it to that of SM (or putting this model in the context of SM, we call it “the SM-like effective potential”), and now T_C is not the true temperature for the phase transition of the system, and it should be called “the SM-like critical temperature.”

As commented earlier in Sec. IIE, when studying phase transitions in 2HDM, studies rarely mention phase transition temperature. Because the analysis of the phase transition temperature of the two VEVs model would be very difficult due to their mixing. As analyzed in this section, the S_3 symmetry separates the two phase transitions, so it makes the determination of the transition temperature more obvious.

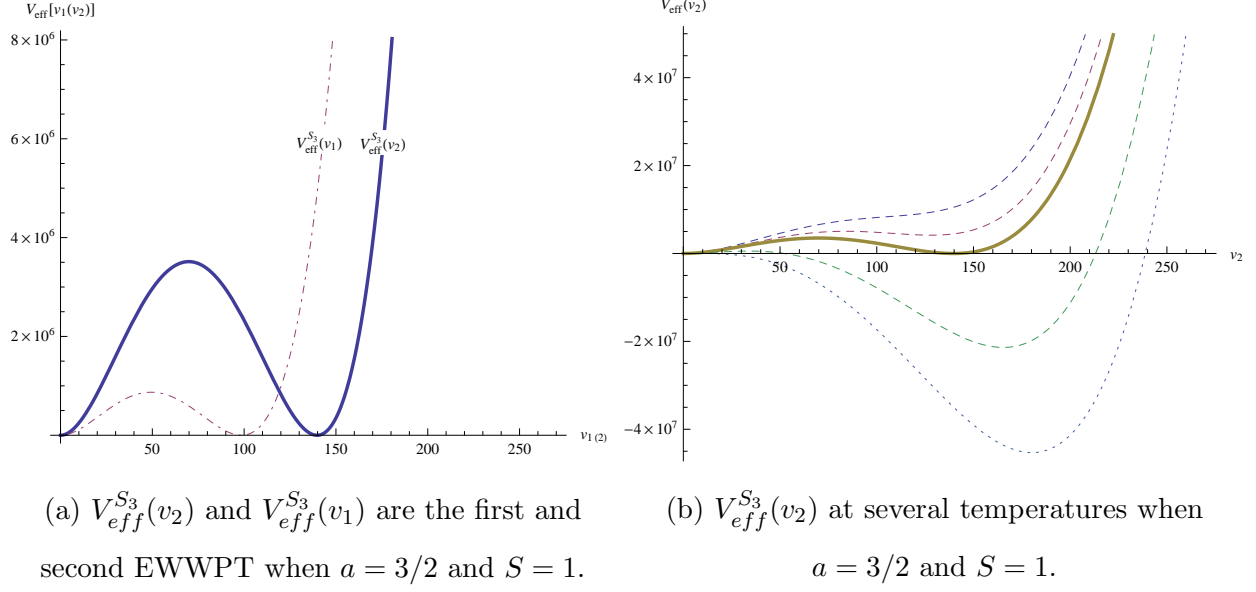


FIG. 6: The effective potential with $a = 3/2$.

Fig. 6b shows us the potential $V_{eff}^{S_3}(v_2)$ at different temperatures. These potentials all have the second non zero minima, with $m_H(v_2) = 150$ GeV, $m_{H^\pm}(v_2) = m_A(v_2) = 302.087$ GeV. The solid line that corresponds to $T_{C1} = 139.739$ GeV, shows that there exists a potential well between the two minima. This is proof of the existence of the first-order in the phase transitions.

In Fig. 6a, the solid line is the shape of $V_{eff}^{S_3}(v_2)$ at $m_H(v_2) = 150$ GeV, $m_{H^\pm}(v_2) = m_A(v_2) = 302.087$ GeV, and $T_{C1} = 139.739$ GeV. The dash-dotted line is $V_{eff}^{S_3}(v_1)$ when $m_H(v_1) = 150/\sqrt{2}$ GeV, $m_{H^\pm}(v_1) = m_A(v_1) = 302.087/\sqrt{2}$ GeV, and $T_{C2} = 98.761$ GeV. The nonzero minimum and maximum of the dash-dotted are smaller than that of the solid line and $T_{C1} > T_{C2}$, which shows that the phase transition must occur in two stages. The distance between the two stages is $\Delta T_C = T_{C1} - T_{C2} = 40.978$ GeV.

To be more intuitively in the comments, we plot the effective potential $V_{eff}^{S_3}(v_2)$ and $V_{eff}(v)$ in case of $a = 2$ as in Fig. 7. The blue solid line is the potential $V_{eff}(v_2)$ when $m_H(v_2) = 140$ GeV, $m_{H^\pm}(v_2) = m_A(v_2) = 272.647$ GeV and the phase transition's temperature $T_{C1} = 124.283$ GeV. The dashed line is for $m_A(v) = 198$ GeV, $m_{H^\pm}(v) = m_A(v) = 362.284$ GeV and the critical temperature is $T_C = 169.288$ GeV.

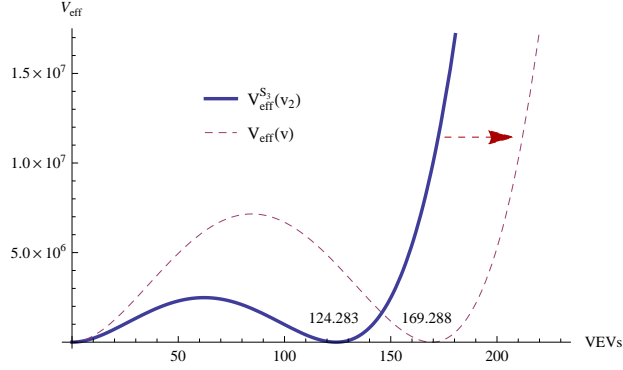


FIG. 7: $V_{eff}^{S_3}(v_2)$ and $V_{eff}(v)$ when $v_1 = v_2$ or $a = 2, \tan \beta = 1$

Through Fig. 7, when $a = 2$, that is when $v_1 = v_2$, the two stages of the EWPT occur at the same time. Each stage of the phase transition is described by the blue solid line. The correct temperature for the phase transition of the system must be T_{C1} .

However, also through Fig. 7, if we describe our system using the composite potential $V_{eff}(v)$, that is if we study the phase transition of the system in just one stage as in SM, the effective potential of the system at the phase transition temperature is as the dashed line. Here the temperatures for the system are $T_C > T_{C1}$. By describing the EWPT in only one stage as in the SM, the two effective potentials were turned in the solid line into the dashed line. Accidentally, this did not change the strength of the phase transition but instead increased the critical phase transition's temperature and VEV, making them different compared to the correct ones.

F. Searching the first-order EWPT and the role of $\tan \beta$

In order to meet a first-order phase transition, the transition strength must have its value bigger or at least equal to 1. However, there are three unknown variables m_A, m_{H^\pm} and m_H in our problem. Therefore we can assume that $m_A \equiv m_{H^\pm}$. This assumption is only intended to reduce the number of variables in the problem and find the domain for the masses of the particles in the first-order phase transition. This assumption should not be applied to the parameters in the Higgs potential. Also assuming that $m_A = m_{H^\pm}$ or $m_H = m_{H^\pm}$, but the results are all the same. Choosing to use $m_A = m_{H^\pm}$ which is consistent with the previous studies and the data for the parameter ρ [108–112].

According to the comments in Sec. II E, especially in Ref. [97], there can be many sugges-

tions between the three quantities m_{H^\pm}, m_H, m_A but it is possible for a first order EWPT, so from the suggestions, we can choose the scenario $m_A = m_{H^\pm}$ in the 2HDM- S_3 model. Because the symmetry S_3 does not lose or add any of the three additional Higgs bosons.

Furthermore, the effective potential without daisy loop is first used to calculate S . Then daisy loops will be additionally calculated later.

From there, the domain for the value of the masses cannot be too broad, in fact, these domains must be closed. Indeed, to have $S > 1$, and if we apply the following conditions altogether: $T_0^2 > 0$ and T_C must be real or according to Eq. (51), $1 - \theta^2/[\gamma\lambda_{T_c}] > 0$, mass domains must be closed. The numerical solution for the case of $a = 3/2$ for the first stage of the phase transition that corresponds to v_2 is given as Fig. 8.

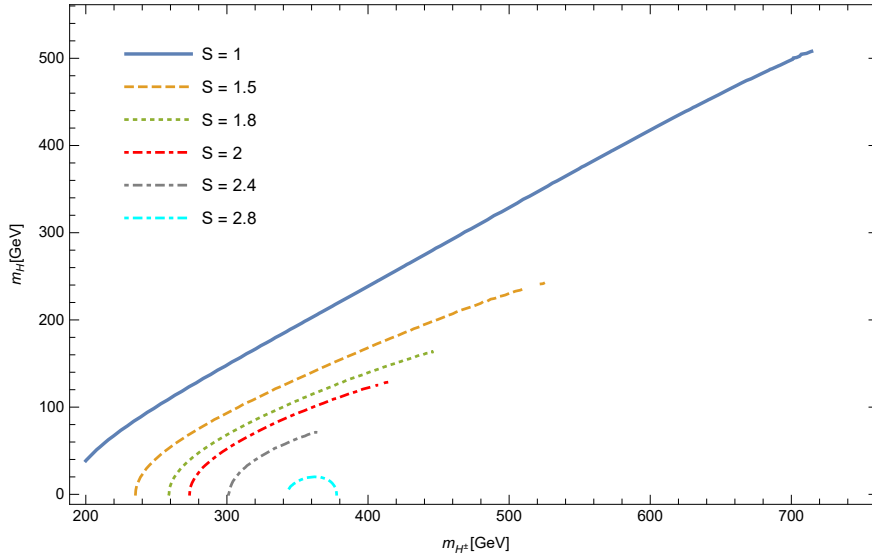


FIG. 8: The strength of first stage EWPT with $a = 3/2$

The contours of $S = 1$ are plotted onto the mass axes and then gradually increase the value of S . With different values of a , a range of values of the phase transition strength was found, $1 \leq S < 2.8$.

Moreover, according to Fig. 8, when S increases, the domain for the masses of the particles must narrow down. Therefore, in order to find these domains for different values of a , only plotting $S = 1$ with different a 's, which is shown in Fig. 9.

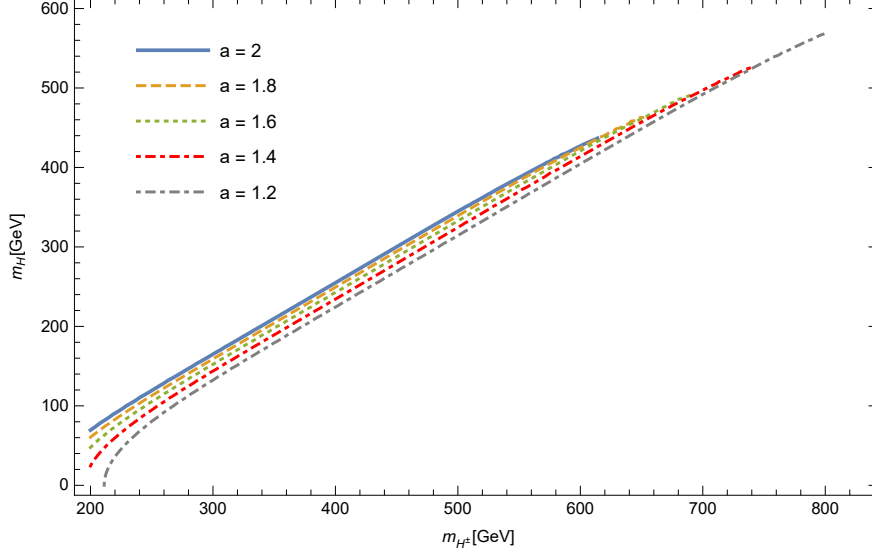


FIG. 9: The mass domain of the particles depends on a with $S = 1$ in the first phase transition

Carefully looking at Fig. 9, when a increases, the mass domains of the particles narrow down. Since $1 < a \leq 2$, the mass domain for each value of a as follows:

$$200 \text{ GeV} < m_{H^\pm}(v_2) < 800 \text{ GeV}, \quad (75)$$

$$0 < m_H(v_2) < 600 \text{ GeV}. \quad (76)$$

The second stage of the phase transition that corresponds to v_1 is similar to the first stage. And because the strength of the phase transition does not depend on a , if the first stage of the phase transition has the transition's strength larger than 1 then so does stage 2. Therefore, the domains for the masses of the particles at stage 2 can be indicated,

$$200 \times \sqrt{(a-1)} \text{ GeV} < m_{H^\pm}(v_1) < 800 \times \sqrt{(a-1)} \text{ GeV}, \quad (77)$$

$$0 < m_H(v_1) < 600 \times \sqrt{(a-1)} \text{ GeV}. \quad (78)$$

Thus, according to Eq. (76) and Eq. (78), although a (or $\tan\beta$) does not affect the phase transition's strength, it affects the domains of the masses of the particles to have the first-order phase transition.

Combining Eqs. (75), (76), (77), (78) together, it follows that

$$200 \times \sqrt{a} \text{ GeV} < m_{H^\pm} < 800 \times \sqrt{a} \text{ GeV}, \quad (79)$$

$$0 < m_H < 600 \times \sqrt{a} \text{ GeV}. \quad (80)$$

Notice that the maximum value of a is 2, it follows from Eqs. (79), (80) that for $a = \sqrt{2}$. So, the maximum value of masses are only increased by about 1.41 times. Therefore, the effect of a on the mass domain of the particles is not too large. This is also easy to see when observing the lines in Fig. 9, they are very close together.

One more thing, if a is closer to 2, the two stages are also closer to each other. Hence, a can be used to define the distance between the two-phase transition stages in this model.

With the analysis of EWPT in 2HDM, the value of $\tan \beta$ is quite wide (from 1 to 17 in all scenarios as indicated in Sec. II E), it is almost a free parameter in the EWPT problem. However, in the 2HDM- S_3 model, due to the S_3 symmetry, the two EWPT stages are separated, thereby highlighting the role of $\tan \beta$ which determines the width of the mass domain as well as the gap between the two stages.

The last important part in this section will be estimating the contribution from daisy loops. Based on Eq. (78), the masses of the exotic Higgs bosons are usually chosen to be larger than the mass of the top quark. This is in keeping with the difficulty of detecting these particles today. Because it only consider the temperature region where EWPT occurs or $\frac{V_c}{T_c} > 1$. So $\frac{m_{A,H,H^\pm}(V_c)}{T_c} \sim 1$, the contribution of daisy loops of exotic Higgs bosons will be small [105]. Thus when adding daisy loops, only the daisy loops of gauge boson and SM-like Higgs boson, i.e., Eqs. (56) are taken into account and neglecting $\Lambda_{h-exotic}$. But notice that, in the temperature region $T \gg T_C$, the contributions from daisy loops of the exotic Higgs bosons cannot be ignored.

Take a look at the graphs in Fig. 10, the red zone indicates the difference between V_{eff} and V_{eff}^{daisy} , the higher the temperature, the larger the difference, and the larger the area of the red region. The phase transition temperatures in this model are similar to SM, they are in the range of 100 to 150 GeV. Because $v = \sqrt{v_1^2 + v_2^2} = 246 \text{ GeV}$ and $v_1, v_2 < 246 \text{ GeV}$. So also from Fig. 10, when $T < 150 \text{ GeV}$, the area of the red region is very small.

Thus, also from Fig. 10, daisy loops will increase the phase transition temperature. Indeed, the second pair of lines in Fig. 10, when $T = 139.739 \text{ GeV}$ is also the phase transition temperature corresponding to V_{eff} (the upper line). But V_{eff}^{daisy} (bottom line) has a second

minimum that is below the VEV axis, so $T = 139.739$ GeV is not yet the phase transition temperature corresponding to V_{eff}^{daisy} , this phase transition temperature must be greater than 139.739 GeV. Finally, a sure result is that as the phase transition temperature increases, the phase transition strength will decrease.

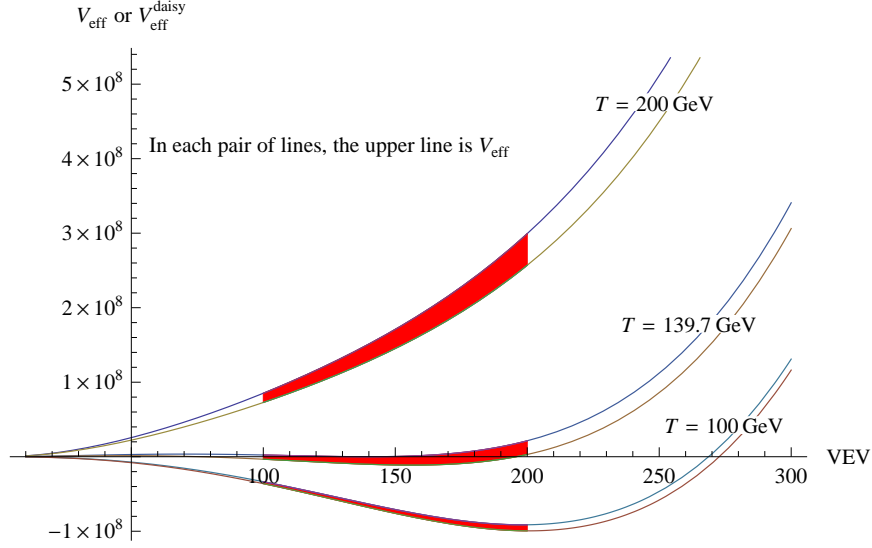


FIG. 10: Difference between V_{eff}^{S3} and V_{eff}^{daisy} with $m_H(v_2) = 150$ GeV, $m_{H^\pm}(v_2) = m_A(v_2) = 302.087$ GeV.

Next to see the effect from daisy loops about S as the above comments. The masses of H^\pm and H are randomly selected, then recalculate S with and without daisy loops, as shown in Table V.

$m_H(v_2)$ [GeV]	$m_{H^\pm}(v_2)$ [GeV]	$S_{nodaisy}$	S_{daisy}	$S_{daisy}/S_{nodaisy}$
300	500	1.116	1.0938	0.979
400	600	1.048	1.030	0.982
250	470	1.253	1.224	0.976
220	430	1.254	1.222	0.974
180	410	1.452	1.410	0.971

TABLE V: Strength S with and without daisy loops

The ring-loops reduce S by 2/3 times [40, 65]. But in this model, this ratio is about 0.97 times or the maximum value of strength is about 2.71. However, this still ensures the

first-order EWPT.

Although the daisy loops do not significantly change the strength of the phase transition in this model, but the role of reducing divergences in effective potential calculations cannot be ignored.

In addition, it should be noted that in this model the triggers for the first order phase transitions are heavy Higgs particles. So the daisy loops of heavy Higgs have no effect in EWPT. However, other models exist light particles besides the SM, surely the daisy loops of these particles will have a great effect on EWPT.

V. CONCLUSION AND OUTLOOKS

The 2HDM- S_3 was chosen to analyze the EWPT stages, not only because it is close to the SM but also because the structure of the EWPT process in this model is interesting enough for us to find new things. Moreover, although these models have some features that are new to the SM, they are far more complicated as they have more new fields and VEVs.

The symmetry breaking process that corresponds to the EWPT in the 2HDM- S_3 , when compared with the SM, is depicted in the below diagram.

$$\begin{array}{c}
2\text{HDM-}S_3 \\
\Downarrow \text{breaking } v_2 \\
\Downarrow \text{breaking } v_1 \\
U(1)_Q
\end{array}$$

We first summarize the structural analysis methods of the EWPT from previous studies along with the method in this article as follows:

- The first method as in Refs. [15, 55]: The EWPT process is considered as in the SM. The effective potential $V_{eff}(v)$ is used and $v^2 = v_1^2 + v_2^2$.
- The second method as in Refs. [95, 97]: Assuming the equation Eq. (A14), examining the multistep EWPT process, and the effective potential is a function of two variables v_1 and v_2 . But when calculating the strength of phase transition $\xi = \frac{v_c}{T_c}$, $v^2 = v_1^2 + v_2^2$, it is still referred to as one phase as the standard model.

- The third method is in this article: Analyzing the division of the effective potential into two separate parts [$V_{eff} = V_{eff}(v_1) + V_{eff}(v_2)$] and examining each stage separately.

The EWPT has been intensively considered in the 2HDM. Some remarks are in order.

In Refs. [113, 114], the EWPT has been considered in the 2HDM type I and II. In these papers, the masses of heavy particles are not larger than 1 TeV and their mass difference is not bigger 400 GeV. In our results, the mass region of heavy particles ranges from 200 to 800 GeV. Therefore, the maximum mass difference between the heavy particles is about 600 GeV. The lattice simulation with one-loop effective potential for crystal has been considered in Ref. [114], the first order EWPT happens for a scenario $m_{H^\pm} = m_A$, and this agrees with our assumption. Therefore, the results in Refs. [113, 114] and ours are compatible.

It was shown that the EWPT is related to a significant uplifting of the Higgs vacuum [115]. The first order phase transition leads to the following condition

$$m_A > m_H + m_Z . \quad (81)$$

The mass domain of particles in our calculation is also compatible with this.

The first order EWPT is possible if $580 \text{ GeV} < m_{H^\pm} < 1 \text{ TeV}$ [116]. This constraint agrees with our result $m_{H^\pm} < 800 \times \sqrt{a} \text{ GeV} \sim 1 \text{ TeV}$ as in Eqs. (79) and (80).

In Ref. [117], the first order EWPT happens in the 2HDM type I and II with the mass difference between H, H^\pm and A in the range (100, 300) GeV. This coincides with the mass region in Eqs. (75) and (76).

From Fig. 1 in Ref. [118] it follows that to have the first order phase transition, the maximal mass difference among m_H and m_A is about 500 GeV. In our study this value is about 600 GeV. Hence, both results are consistent.

In Ref. [119], Fig. 3, the effective potential is plotted in the region of masses lower than 600 GeV and the value of $\tan \beta$ runs from 1 to 20. The lines of the effective potential for different $\tan \beta$ values are very close to each other. The result shows that S is almost independent on $\tan \beta$, and this supports our conclusion.

All three methods are acceptable approximations. The effectiveness of the third method in this article is clearly stated in Sec. IV. Mathematical techniques for analyzing VEVs in the first and second method have been successfully used to analyze decay channels in multi-VEV models [120, 121].

Exploring the EWPT process into several stages has been analyzed in many other models besides 2HDM, as shown in Refs. [74, 122]. Therefore, the results of this paper aim to emphasize the feature of the multiphase in 2HDM- S_3 model and investigate the factors that affect the division of stages as well as the influence of $\tan \beta$.

The strength of the phase transition does not depend on a or $\tan \beta$, and to study the full structure of the two stages of the phase transition, the effective potential must not be written as $V_{eff}(v)$. The greater $\tan \beta$ is, the narrower the mass domain of the particles in the first order of the phase transition becomes. The S_3 symmetry has shown that there are two subsequential stages in the phase transition process, which has not been shown clearly in the 2HDM where there are many mixing terms of the VEVs in the mass domain of the particles.

The S_3 symmetry could explain the mixing of quarks or this symmetry could be related to the Yukawa couplings that can affect EWPT processes [76–78]. For example in Ref. [123], changing the Yukawa coupling constants results in a first order EWPT. Therefore, the S_3 symmetry associated with the quark mixing has an effect on EWPT processes that need to be further elucidated after these works.

By analyzing the effect of daisy loops, a way of assessing the contribution from daisy loops: first the EWPT was calculated by using the effective potential without daisy loops, to estimate the mass domain of particles; then based on that mass domain, estimating the ratio $m(v)/T$ to consider the contribution from daisy loops.

In this paper, in order to reduce the number of variables in our problem, $m_A = m_{H^\pm}$ has been assumed. As said earlier, this assumption was only made to find the mass domain of the particles, and must not be applied to the parameters in the Higgs potential, since the real values of these 2 particles can be different from each other, even though their domains of mass can be identical. However, from Eq. (40) and this assumption, $l_3 \approx 0$. This assumption was made by the authors in order to satisfy the data of the parameter ρ in the 2HDM [108–112] so that if the 2HDM- S_3 also satisfies the data of the parameter ρ , this can lead to l_3 being very small. This is one of the results of this paper that can lead to research on the parameter ρ in the 2HDM- S_3 .

As stated in remark 4, the assessment of the impact the first stage of EWPT has on the second stage of EWPT is made through the mixing terms of the VEVs. However, the investigation of the effects of κ is still unclear. All these effects of κ have been renormalized

under the minimum conditions of the later EWPT stage. Therefore, from remark 4, to assess the effects of κ , we must rebuild the whole effective potential that contains the mixing terms of VEVs all over. Assessing this direction is a new incoming, and interesting job after this paper.

Notice the comments in the Sec. II E, we focus on scalar decays into heavy fermions ($A, H, H^\pm \rightarrow tt, tb$), which are the most promising channels for demonstrating the first-order EWPT through confirmation of additional bosons [124]. Also, there is another way to check, we can measure the gravitational waves generated by the EWPT process in future experiments by LISA [124].

Finally, through the comments on effective potentials, writing down the effective potentials in the form of $V_{eff}(v)$ is imprecise, but still, it is concise and gives accurate predictions for the strength of the phase transition. However, there will be some small errors in calculating the corresponding sphaleron energy, but these errors would not be large. Since the contributions of the effective potential term in the sphaleron energy are quite small, about 5.5% [125], when writing down the effective potential of the system in the form of $V_{eff}(v) = \frac{a^2}{(a-1)^2+1} V_{eff}^{S_3}$, this will make the sphaleron energy deviate by about 5.5%. From this, to make the calculation of the sphaleron become more accurate, we only need to replace $V_{eff}(v)$ by $\frac{(a-1)^2+1}{a^2} V_{eff}(v)$, and the methods are still the same as in Refs. [55, 56, 126, 127]. In addition, if the two stages of the phase transition in this model occur at the same time or very close to each other, the bubbles of each of the phase transition stages can collide with each other or collide with the bubbles from other stages, thereby causing some big gravitational waves. For that matter, the full estimation of the contributing terms, as well as the impact of the ratio $\frac{(a-1)^2+1}{a^2}$ on the sphaleron energy for the gravitational wave calculation, will be the extension of this paper.

The method of high-temperature dimensional reduction to the 2HDM to obtain three-dimensional effective theories that can be used for nonperturbative simulations [128]. These results can be used to recalculate EWPT in 2HDM, and to check our results. This is part of the upcoming work.

ACKNOWLEDGMENTS

V.Q.P. would like to thank Pham Quang Khanh for reading and editing the article in English and running my small code. H. N. L. is thankful to Van Lang University.

Appendix A: Effective action of multiscalar field models

In the ϕ^4 theory and the single field case, calculating the effective potential from summing the diagrams is shown in Ref. [91]. Let us consider a toy model described by two neutral scalar fields $(\phi_i, i = 1, 2)$ with an action

$$S(\phi_1, \phi_2) = \int d^4x \mathcal{L}(\phi_1(x), \phi_2(x)), \quad (\text{A1})$$

where

$$\mathcal{L}(\phi_1(x), \phi_2(x)) = \sum_{i=1}^2 (\partial_\mu \phi_i^* \partial^\mu \phi_i - m_{\phi_i}^2 \phi_i^* \phi_i) - \frac{\lambda_\phi}{4} (\phi_1^* \phi_1 + \phi_2^* \phi_2)^2 \quad (\text{A2})$$

In the path-integral representation, the generating functional is as the following:

$$Z[J] = \langle 0_{\text{out}} | 0_{\text{in}} \rangle_J \equiv \int \mathcal{D}\phi_1 \mathcal{D}\phi_2 \exp\{i(S(\phi_1, \phi_2) + \phi_1 J_1 + \phi_2 J_2)\}, \quad (\text{A3})$$

and

$$Z[J] \equiv \exp\{iW[J]\}, \quad (\text{A4})$$

in which

$$\phi_i J_i \equiv \int d^4x \phi_i(x) J_i(x); \quad i = 1, 2. \quad (\text{A5})$$

The effective action $\Gamma[\bar{\phi}_1, \bar{\phi}_2]$ is the Legendre transform of Eq. (A4)

$$\Gamma[\bar{\phi}_1, \bar{\phi}_2] = W[J] - \sum_{i=1}^2 \int d^4x \frac{\Delta W[J]}{\Delta J_i(x)} J_i(x) \quad (\text{A6})$$

where the VEVs of ϕ_i are

$$\bar{\phi}_i(x) = \frac{\delta W[J]}{\delta J_i(x)} \quad (\text{A7})$$

From Eq. (A6) and Eq. (A7), the generating functionals can be obtained

$$\frac{\delta \Gamma[\bar{\phi}_1, \bar{\phi}_2]}{\delta \bar{\phi}_i} = \frac{\delta W[J]}{\delta J_i} \frac{\delta J_i}{\delta \bar{\phi}_i} - J_i - \bar{\phi}_i \frac{\delta J_i}{\delta \bar{\phi}_i} = -J_i. \quad (\text{A8})$$

where using of the notation from Eq. (A5). Eq. (A8) implies in particular that

$$\left. \frac{\delta \Gamma[\bar{\phi}_1, \bar{\phi}_2]}{\delta \bar{\phi}_i} \right|_{J_i=0} = 0. \quad (\text{A9})$$

$Z[J]$ can be expanded in a power series of J and in terms of Green functions $G_{(n)}$ as

$$Z[J] = \sum_{n=0}^{\infty} \frac{i^n}{n!} \int d^4 x_1 \dots d^4 x_n J(x_1) \dots J(x_n) G_{(n)}(x_1, \dots, x_n) \quad (\text{A10})$$

and

$$iW[J] = \sum_{n=0}^{\infty} \frac{i^n}{n!} \int d^4 x_1 \dots d^4 x_n J(x_1) \dots J(x_n) G_{(n)}^c(x_1, \dots, x_n). \quad (\text{A11})$$

However, in the next step, expanding the effective action in terms of the one-particle irreducible Green functions ($\Gamma^{(n)}$),

$$\Gamma[\bar{\phi}_1, \bar{\phi}_2] = \sum_{n=0}^{\infty} \frac{1}{n!} \int d^4 x_1 \dots d^4 x_n \bar{\phi}_1(x_1) \dots \bar{\phi}_1(x_{n_1}) \bar{\phi}_2(x_{n_1+1}) \dots \bar{\phi}_2(x_{n_2}) \Gamma^{(n)}(x_1, \dots, x_n). \quad (\text{A12})$$

The number of vertices n_1 and n_2 are arbitrary but $n_1 + n_2 = 2n$. We compute $\Gamma^{(n)}(p_i = 0)$ which are the diagrams with $2n$ external lines. Analyzing this in detail with the case of one-loop as shown Fig. 11 which is represented by the formula:

$$\Gamma_n(\phi_{1c}, \phi_{2c}) = i \frac{1}{2n} \int \frac{d^4 p}{(2\pi)^4} \left(\frac{i}{p^2 - m^2(\phi_{1c}, \phi_{2c}) + i\varepsilon} \right)^n (-i\lambda_{\phi_1})^{n_1/2} (\phi_{1c})^{n_1} (-i\lambda_{\phi_2})^{n_2/2} (\phi_{2c})^{n_2}. \quad (\text{A13})$$

In Eq. (A13), each vertex is a factor $-i\lambda_{\phi_i}$, the external line is the factor $\bar{\phi}_i = \phi_{ic} = \text{const.}$ The above integral is easy to calculate if the external lines are of the same type (i.e., $n_1 = 0$ or $n_2 = 0$). However, when both n_1 and n_2 are nonzero, i.e., the external lines have both fields, calculating the above integral is not simple. Also then summing with $n = 0$ to infinity, it is unlikely that this infinite sum converges. So in general, 1-loop contributions cannot be represented as

$$V_1(\phi_{1c}, \phi_{2c}) = \frac{1}{2} \int \frac{d^4 p}{(2\pi)^4} \log [p^2 + m^2(\phi_{1c}, \phi_{2c})]. \quad (\text{A14})$$

The representation of one-loop contribution like the above result is only a stereotype application from the calculation results of the single-field case (i.e., from the result, $V_1(u_c) =$

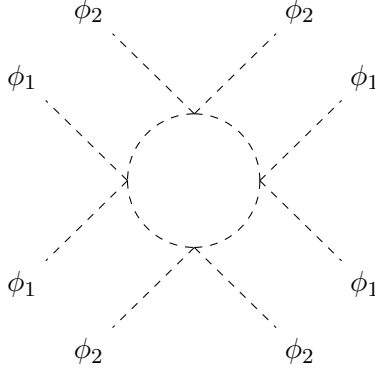


FIG. 11: The 1-loop diagram with the ϕ_1 and ϕ_2 external lines

$\frac{1}{2} \int \frac{d^4 p}{(2\pi)^4} \log [p^2 + m^2(u_c)]$ in Ref. [91], u_c is VEV of single scalar field). But the computation of the diagrams has been ignored. Although this is imprecise, if we unconditionally accept the one-loop contributions as Eq. (A14), it is also a fairly general estimate of one-loop contributions when considering two fields at once. This is also a possible method today in the context of calculation Eq. (A13). Nevertheless, it is very difficult.

However, this representation is also true, if we interpret the above result as implying $\phi_{2c} = \kappa \phi_{1c}$, that is, the above result represents only one field ϕ_1 or ϕ_2 ; or ignoring all the diagrams where ϕ_1 and ϕ_2 are present at the same time. Therefore $V_1(\phi_{1c}, \phi_{2c}) \equiv V_1(\phi_c)$ with $\phi_c^2 = \phi_{1c}^2 + \phi_{2c}^2$. This is a very good approximation that eliminates the difficulty of summing diagrams as shown in Fig. 5. This approximation has been used in calculating decay channels or diagrams as in Refs. [129–131]. Also, there are basis-independent methods for the two-Higgs-doublet model [88, 124], it is possible to rewrite 2HDM model under one VEV. But in the sections of article, this approximation is only imprecise in the EWPT analysis.

The next interesting thing here is what if we could rewrite $\mathcal{L}(\phi_1(x), \phi_2(x)) = \mathcal{L}(\phi_1(x)) + \mathcal{L}(\phi_2(x))$, when expanding ϕ_i in terms of ϕ_{ic} . At that point, the generating functional is rewritten as

$$Z[J] = Z[J_1].Z[J_2], \quad (\text{A15})$$

so that,

$$W[J] = W[J_1] + W[J_2]. \quad (\text{A16})$$

In other words, the effective potential can be separated into two separate parts:

$$\Gamma[\bar{\phi}_1, \bar{\phi}_2] = W[J] - \int d^4x \frac{\delta W[J]}{\delta J_i(x)} J_i(x) \quad (\text{A17})$$

$$= W[J_1] - \int d^4x \frac{\delta W[J_1]}{\delta J_1(x)} J_1(x) + W[J_2] - \int d^4x \frac{\delta W[J_2]}{\delta J_2(x)} J_2(x) \quad (\text{A18})$$

$$= \Gamma[\bar{\phi}_1] + \Gamma[\bar{\phi}_2] \quad (\text{A19})$$

This will make summing the diagrams easier, but they are not always separated like that. The cases of more than two fields are similarly constructed.

-
- [1] A. D. Sakharov, JETP Lett. **5**, 24 (1967).
 - [2] M. I. Dine, R. G. Leigh, P. Huet, A. Linde, and D. Linde, Phys. Rev. D **46**, 550 (1992).
 - [3] K. Kajantie, M. Laine, K. Rummukainen, and M. Shaposhnikov, Phys. Rev. Lett. **77**, 2887 (1996).
 - [4] F. Csikor, Z. Fodor, and J. Heitger, Phys. Rev. Lett. **82**, 21 (1999).
 - [5] J. Grant and M. Hindmarsh, Phys. Rev. D **64**, 016002 (2001).
 - [6] M. D’Onofrio, K. Rummukainen and A. Tranberg, J. High Energy Phys. **08** (2012) 123.
 - [7] M. D’Onofrio, K. Rummukainen, and A. Tranberg, Phys. Rev. Lett. **113**, 141602 (2014).
 - [8] Vo Quoc Phong, Vo Thanh Van, and Hoang Ngoc Long, Phys. Rev. D **88**, 096009 (2013).
 - [9] A. Menon, D. E. Morrissey, and C. E. M. Wagner, Phys. Rev. D **70**, 035005 (2004).
 - [10] S. W. Ham, S. K. Oh, C. M. Kim, E. J. Yoo, and D. Son, Phys. Rev. D **70**, 075001 (2004).
 - [11] M. Bastero-Gil, C. Hugonie, S. F. King, D. P. Roy, and S. Vempati, Phys. Lett. B **489**, 359 (2000).
 - [12] A. Menon, D. E. Morrissey, and C. E. M. Wagner, Phys. Rev. D **70**, 035005 (2004).
 - [13] J. M. Cline, G. Laporte, H. Yamashita and S. Kraml, J. High Energy Phys. **0907** (2009) 040.
 - [14] A. Azatov and M. Vanvlasselaer, J. High Energy Phys. **09** (2020) 085.
 - [15] S. Kanemura, Y. Okada, and E. Senaha, Phys. Lett. B **606**, 361 (2005).
 - [16] G. C. Dorsch, S. J. Huber, and J. M. No, J. High Energy Phys. **10** (2013) 029.
 - [17] S. W. Ham, S-A Shim, and S. K. Oh, Phys. Rev. D **81**, 055015 (2010).
 - [18] D. Borah and J. M. Cline, Phys. Rev. D **86**, 055001 (2012).

- [19] A. Ahriche and S. Nasri, Phys. Rev. D **85**, 093007 (2012).
- [20] S. Das, P. J. Fox, A. Kumar, and N. Weiner, J. High Energy Phys. **1011** (2010) 108.
- [21] D. Chung and A. J. Long, Phys. Rev. D **84**, 103513 (2011).
- [22] M. Carena, N. R. Shaha, and C. E. M. Wagner, Phys. Rev. D **85**, 036003 (2012).
- [23] V. Q. Phong, H. N. Long, V. T. Van, and N. C. Thanh, Phys. Rev. D **90**, 085019 (2014).
- [24] J. Sá Borges and R. O.Ramos, Eur. Phys. J. C **76**, 344 (2016).
- [25] V. Q. Phong, H. N. Long, V. T. Van, and L. H. Minh, Eur. Phys. J. C **75**, 342 (2015).
- [26] J. R. Espinosa, T. Konstandin, and F. Riva, Nucl. Phys. **B854**, 592 (2012).
- [27] S. Kanemura, E. Senaha, T. Shindou, and T. Yamada, J. High Energy Phys. **1305** (2013) 066.
- [28] D. J. H. Chung and A. J. Long, Phys. Rev. D **81**, 123531 (2010).
- [29] G. Barenboim and N. Rius, Phys. Rev. D **58**, 065010 (1998).
- [30] S. Profumo, M. J. Ramsey-Musolf, and G. Shaughnessy, J. High Energy Phys. **0708** (2007) 010.
- [31] S. Profumo, M. J. Ramsey-Musolf, C. L. Wainwright, and P. Winslow, Phys. Rev. D **91**, 035018 (2015).
- [32] D. Curtin, P. Meade, and C-T. Yu, J. High Energy Phys. **11** (2014) 127.
- [33] M. Jiang, L. Bian, W. Huang, and J. Shu, Phys. Rev. D **93**, 065032 (2016).
- [34] M. Carena, G. Nardini, M. Quiros, and C. E.M. Wagner, Nucl. Phys. **B812**, 243 (2009).
- [35] A. Katz, M. Perelstein, M. J. Ramsey-Musolf, and P. Winslow, Phys. Rev. D **92**, 095019 (2015).
- [36] J. Kozaczuk, S. Profumo, L. S. Haskins, C. L. Wainwright, J. High Energy Phys. **1501** (2015) 144.
- [37] H. H. Patel and M. J. Ramsey-Musolf, Phys. Rev. D. **88**, 035013 (2013).
- [38] N. Blinov, J. Kozaczuk, D. E. Morrissey, and C. Tamarit, Phys. Rev. D **92**, 035012 (2015).
- [39] S. Inoue, G. Ovanessian, and M. J. Ramsey-Musolf, Phys. Rev. D **93**, 015013 (2016).
- [40] H. H. Patel and M. J. Ramsey-Musolf, J. High Energy Phys. **1107** (2011) 029.
- [41] G. W. Anderson and L. J. Hall, Phys. Rev. D **45**, 2685 (1992).
- [42] H. H. Patel, M.J. Ramsey-Musolf, M. Garny and T. Konstandin, J. High Energy Phys. **1207** (2012) 189.
- [43] J. De Vries, M. Postma, and J. van de Vis, J. High Energy Phys. **1904** (2019) 024.

- [44] J. de Vries, M. Postma, J. van de Vis , G. White, J. High Energy Phys. **1801** (2018) 089.
- [45] C. Balazs, G. White, and J. Yue, J. High Energy Phys. **1703** (2017) 030.
- [46] A. Ahriche, Phys. Rev. D **75**, 083522 (2007).
- [47] A. Ahriche, Eur. Phys. J. C **66**, 333 (2010).
- [48] T. A. Chowdhury and S. Nasri, J. High Energy Phys. **1411** (2014) 096.
- [49] A. Ahriche and S. Nasri, J. Cosmol. Astropart. Phys. **07** (2013) 035.
- [50] A. Ahriche, G. Faisel, S. Y. Ho, S. Nasri and J. Tandean, Phys. Rev. D **92**, 035020 (2015).
- [51] A. Ahriche, K. L. McDonald and S. Nasri, Phys. Rev. D **92**, 095020 (2015).
- [52] A. Ahriche, S. M. Boucenna and S. Nasri, Phys. Rev. D **93**, 075036 (2016).
- [53] A. Ahriche, K. Hashino, S. Kanemura and S. Nasri, Phys. Lett. B **789**, 119 (2019).
- [54] K. Fuyuto and E. Senaha, Phys. Rev. D **90**, 015015 (2014).
- [55] K. Fuyuto and E. Senaha, Phys. Lett. B **747**, 152 (2015).
- [56] K. Funakubo and E. Senaha, Phys. Rev. D **79**, 115024 (2009).
- [57] M. Spannowsky and C. Tamarit, Phys. Rev. D **95**, 015006 (2017).
- [58] C. Grojean, G. Servant, and J. D. Wells, Phys. Rev. D **71** 036001 (2005).
- [59] C. Delaunay, C. Grojean, J. D. Wells, J. High Energy Phys. **0804** (2008) 029.
- [60] A. Kusenko, L. Pearce, and L. Yang, Phys. Rev. Lett. **114**, 061302 (2015).
- [61] V. Q. Phong, H. N. Long, V. T. Van, and L. H. Minh, Eur. Phys. J. C **75**, 342 (2015).
- [62] C. W. Chiang and T. Yamada, Phys. Lett. B **735**, 295 (2014).
- [63] V. Q. Phong, N. C. Thao, and H. N. Long, Phys. Rev. D **97**, 115008 (2018).
- [64] J. R. Espinosa, T. Konstandin, J. M. No and M. Quiros, Phys. Rev. D **78**, 123528 (2008).
- [65] D. Comelli and J.R. Espinosa, Phys.Rev. D **55**, 6253 (1997).
- [66] M. Joyce, Phys. Rev. D **55**, 1875 (1997).
- [67] K. Funakubo and E. Senaha, Phys. Rev. D **79**, 115024 (2009).
- [68] M. Dvornikov and V. B. Semikoz, Phys. Rev. D **87**, 025023 (2013).
- [69] T. M. Gould and I. Z. Rothstein, Phys. Rev. D **48**, 5917 (1993).
- [70] S. Braibant, Y. Brihaye and J. Kunz, Int. J. Mod. Phys. A **08**, 5563 (1993).
- [71] Vo Quoc Phong, Phan Hong Khiem, Ngo Phuc Duc Loc, and Hoang Ngoc Long, Phys. Rev. D **101**, 116010 (2020).
- [72] A. Braconi, Mu-Chun Chen, and G. Gaswint, Phys. Rev. D **100**, 015032 (2019).
- [73] I. Baldes, T. Konstandin, and G. Servant, Phys. Lett. B **786**, 373 (2018).

- [74] Vo Quoc Phong, N. T. Tuong, N. C. Thao, and H. N. Long, Phys. Rev. D **99**, 015035 (2019).
- [75] Vo Quoc Phong and Nguyen Minh Anh, Int. J. Mod. Phys. A **34**, 1950073 (2019).
- [76] D. Das, U. K. Dey, and Palash B. Pal, Phys. Rev. D **96**, 031701 (2017).
- [77] D. Das and U. K. Dey, Phys. Rev. D **89**, 095025 (2014); **91**, 039905(E) (2015).
- [78] D. Das, U. K. Dey and Palash B. Pal, Phys. Lett. B **753**, 315 (2016).
- [79] R. N. Mohapatra and S. Nussinov, Phys. Rev. D **60**, 013002 (1999).
- [80] T. Kitabayashi and M. Yasue, Phys. Rev. D **67**, 015006 (2003).
- [81] W. Grimus and L. Lavoura, Phys. Lett. B **572**, 189 (2003).
- [82] Y. Koide, Phys. Rev. D **69**, 093001 (2004).
- [83] P. F. Harrison and W.G. Scott, Phys. Lett. B **557**, 76 (2003).
- [84] R. N. Mohapatra, S. Nasri, and Yu. Hai-Bo, Phys. Lett. B **639**, 318 (2006).
- [85] J. Barranco and F. Gonzalez Canales, A. Mondragon, Phys. Rev. D **82**, 073010 (2010).
- [86] F. González Canales, A. Mondragón, M. Mondragón, U.J. Saldaña Salazar, L. Velasco-Sevilla, Phys. Rev. D **88**, 096004 (2013).
- [87] D. Cogollo and J. P. Silva, Phys. Rev. D **93**, 095024 (2016).
- [88] S. Davidson and H. E. Haber, Phys. Rev. D **72**, 035004 (2005); **72**, 099902(E) (2005).
- [89] J. Herrero-García, T. Ohlsson, S. Riad and J. Wirén, J. High Energy Phys. **04** (2017) 130.
- [90] G. C. Branco, P. M. Ferreira, L. Lavoura, M. N. Rebelo, Marc Sher, Joao P. Silva, Phys. Rep. **516**, 1 (2012).
- [91] M. Quiros, *Proc. ICTP Summer School in High-Energy Physics and Cosmology (1999)*, p. 187, arXiv:hep-ph/9901312.
- [92] A. Arbey, F. Mahmoudi, O. Stal, and T. Stefaniak, Eur. Phys. J. C **78**, 182 (2018).
- [93] W. Mader, Jae-hyeon Park, G. M. Pruna, D. Stöckinger, and A. Straessner, J. High Energy Phys. **1209** (2012) 125.
- [94] D. Das and Palash B. Pal, Phys. Rev. D **98**, 115001 (2018).
- [95] M. Aoki, T. Komatsu, and H. Shibuya, Prog. Theor. Exp. Phys. **2022**, 063B05.
- [96] V. Khachatryan *et al*, Phys. Lett. B **758**, 296 (2016).
- [97] D. Gonçalves, A. Kaladharan, and Y. Wu, Phys. Rev. D **105**, 095041 (2022).
- [98] G. C. Dorsch, S. J. Huber, and J. M. No, J. High Energy Phys. **10** (2013) 029.
- [99] N. Blinov, S. Profumo, and T. Stefaniak, J. Cosmol. Astropart. Phys. **07** (2015) 028.
- [100] J. O. Andersen, T. Gorda, A. Helset, L. Niemi, T. V. I. Tenkanen, A. Tranberg, A. Vuorinen,

- and D. J. Weir, Phys. Rev. Lett. **121**, 191802 (2018).
- [101] K. Enomoto, S. Kanemura, and Y. Mura, J. High Energy Phys. **01** (2022) 104.
 - [102] Y. Kajiyama, H. Okada, and K. Yagyu, Nucl. Phys. **B887**, 358 (2014).
 - [103] E. Ma, Non-Abelian discrete family symmetries for leptons and quarks, arXiv:hep-ph/0409075.
 - [104] E. Ma and B. Melic, Phys. Lett. B **725**, 402 (2013).
 - [105] M. E. Carrington, Phys. Rev. D **45**, 2933 (1992).
 - [106] D. Curtin and P. Meade, H. Ramani, Eur. Phys. J. C **78**, 787 (2018).
 - [107] A. Katz and M. Perelstein, J. High Energy Phys. **07** (2014) 108.
 - [108] H. E. Haber and A. Pomarol, Phys. Lett. B **302**, 435 (1993).
 - [109] P. H. Chankowski, M. Krawczyk, and J. Zochowski, Eur. Phys. J. C **11**, 661 (1999).
 - [110] J.-M. Gerard and M. Herquet, Phys. Rev. Lett. **98**, 251802 (2007).
 - [111] W. Grimus, L. Lavoura, O.M. Ogreid, and P. Osland, Nucl. Phys. **B801**, 81 (2008).
 - [112] S. de Visscher, J.M. Gerard, M. Herquet, V. Lemaitre, and F. Maltoni, J. High Energy Phys. **0908** (2009) 042.
 - [113] P. Basler, M. Krause, M. M"uhlleitner, J. Wittbrodta, and A. Wlotzkaa, J. High Energy Phys. **12** (2017) 086.
 - [114] J. Bernon, L. Biana, and Y. Jiang, J. High Energy Phys. **05** (2018) 151.
 - [115] G. C. Dorsch, S. J. Huber, K. Mimasub, and J.M. Nob, J. High Energy Phys. **02** (2017) 121.
 - [116] P. Basler, M. M"uhlleitnera, and J. Wittbrodt, J. High Energy Phys. **03** (2018) 061.
 - [117] K. Kainulainen, V. Keus, L. Niemi, K. Rummukainen, T. V.I. Tenkanenc, and V. Vaskonend, J. High Energy Phys. **06** (2019) 075.
 - [118] Wei Su, A. G. Williams, and M. Zhang, J. High Energy Phys. **04** (2021) 219.
 - [119] R. Zhou and L. Bian, Phys. Lett. B **829**, 137105 (2022).
 - [120] H. T. Hung, T. T. Hong, H. H. Phuong, H. L. T. Mai, and L. T. Hue, Phys. Rev. D **100**, 075014 (2019).
 - [121] A. Alves, E. Ramirez Barreto, A. G. Dias, C. A. de S. Pires, F. S. Queiroz, and P. S. Rodrigues da Silva, Phys. Rev. D **84**, 115004 (2011).
 - [122] J. Sa Borges and Rudnei O. Ramos, Eur. Phys. J. C **76**, 344 (2016).
 - [123] A. Braconi, Mu-Chun Chen, Geoffrey Gaswint, Phys. Rev. D **100**, 015032 (2019).
 - [124] S. Kanemura, M. Takeuchi, and K. Yagyu, Phys. Rev. D **105**, 115001 (2022).

- [125] Vo Quoc Phong, Nguyen Chi Thao, and Hoang Ngoc Long, Eur. Phys. J. C **82**, 1005 (2022).
- [126] N. S. Manton, Phys. Rev. D **28**, 2019 (1983).
- [127] F. R. Klinkhamer and N.S. Manton, Phys. Rev. D **30**, 2212 (1984).
- [128] T. Gorda, A. Helset, L. Niemi, T. V. I. Tenkanena, and D. J. Weira, J. High Energy Phys. **02** (2019) 081.
- [129] T. Kon, T. Nagura, and T. Ueda, K. Yagyu, Phys. Rev. D **99**, 095027 (2019).
- [130] Z. Liu and Pei-Hong Gu, Nucl. Phys. B**915**, 206 (2017).
- [131] A. Arhrib, R. Benbrik, Chuan-Hung Chen, R. Guedes, and R. Santos, J. High Energy Phys. **08** (2009) 035.